

POLITECNICO DI TORINO
Master's Degree in Aerospace Engineering



**Politecnico
di Torino**

Master's Degree Thesis

**Preliminary design of an arcjet in the
1kW class for space application**

Supervisors

Prof. Lorenzo CASALINO

Co-supervisors

Ing. Marco MANENTE

Candidate

Ivana ALLOCCA

December 2021

POLITECNICO DI TORINO

Master's Degree in Aerospace Engineering



**Politecnico
di Torino**



Master's Degree Thesis

Preliminary design of an arcjet in the 1kW class for space application

Supervisors

Prof. Lorenzo CASALINO

Candidate

Ivana ALLOCCA

Co-supervisors

Ing. Marco MANENTE

December 2021

Alla mia famiglia.

Summary

The thesis work was undertaken in collaboration with T4i-Technology for propulsion and innovation S.p.A. of Padova. The analysis of the electric propulsion background made it possible to identify the arcjet thruster as an excellent trade-off between the characteristics and performance of other devices. The high thrust-to-weight ratio, good specific impulse values, shorter implementation time of a collision avoidance maneuver for the readiness to reach a certain Δv compared to any other electric thruster are the strengths of this technology and the project is made even more promising by the choice of using a green propellant such as the water. The expected performances are evaluated by implementing a simplified analytical model that is suitable for this preliminary design which has been defined in the perspective of an IOD.

Table of Contents

List of Figures	VIII
List of Tables	X
Symbols	XI
Acronyms	XII
1 Introduction	1
2 Electric Propulsion and Arcjet	3
2.1 Arcjet typical parameters	4
2.2 Arcjet application and maneuver	13
2.3 Propulsion strategy: Comparison with similar thruster	16
3 Arcjet detailed description	21
3.1 Propellant analysis	21
3.2 Electrode and material	28
3.3 Adopted model description	31
3.4 Preliminary schematic design	39
3.5 Expected performance for the designed solution	42
4 Preliminary design	45
4.1 Preliminary design of a dedicated IOD satellite	45
4.2 Evaporator	51
4.3 Tank	55
4.4 Thermal control	59
4.5 Power supply subsystem	60
5 Conclusions	63
Bibliography	65

List of Figures

2.1	Representation of an arcjet system	5
2.2	Characteristic voltage-current [1]	6
2.3	Operating modes of the arcjet thruster [2]	7
2.4	Electric arc subject to magnetic forces [1]	8
2.5	Magnetic field across the radial direction [1]	8
2.6	Pressure across the radial direction [1]	9
2.7	Instability of the electric arc [1]	10
2.8	Voltage and electric field between the electrodes [1]	11
2.9	A generic electric thruster [1]	11
2.10	Optimal specific impulse [3]	14
2.11	Performance comparison of chemical thruster and EP [3]	19
3.1	The effect of dissociation on the enthalpy of hydrogen [5]	22
3.2	Theoretical variation of frozen flow efficiency with specific impulse for Hydrogen at various pressures [5]	22
3.3	Variation of specific heat at constant pressure with temperature for hydrogen, ammonia, helium, hydrazine, argon	25
3.4	Variation of specific impulse with chamber temperature for hydrogen, ammonia, helium, hydrazine, argon	26
3.5	Computed isotherms within the gas region and the solid region [6] .	27
3.6	Electrical resistivity of ceramic materials [7]	30
3.7	Thermal conductivity of ceramic materials [7]	30
3.8	Representation of the dual channel model [9]	32
3.9	Representation of the electric arc growth [9]	38
3.10	Geometry of nozzle	40
4.1	CubeSats size	47
4.2	Satellite subsystems assembly	49
4.3	Typical heat-transfer regimes for boiling in flow channel [14]	51
4.4	Sketch of propellant feed system	52
4.5	Vaporizer Concept for Ammonia [15]	53

4.6	Gas generator adopted by Talos arcjet [15]	53
4.7	Prototype of gas generator for water [16]	54
4.8	Skech of gas generator concept [16]	54
4.9	Blowdown system [17]	56
4.10	Section of spherical tank	57
4.11	Voltage-current characteristics of arc and PPU. [1]	61

List of Tables

2.1	Characteristic of main EP thruster types [4]	16
2.2	Typical Δv value required in space missions [3]	18
3.1	Characteristics of various metals [7]	28
3.2	Geometria	40
3.3	Geometry variation parameter	42
3.4	Performance data of nozzles 1 and 2	42
3.5	Performance data of nozzles 1 and 3, $\dot{m} = 23mg/s$, $I = 10A$	43
3.6	Performance data of nozzles 3 and 4, $\dot{m} = 18mg/s$, $I = 10A$	43
3.7	Geometric arameters of the arcjet	44
4.1	Definition of the Technical Readiness Level TRL [11]	46
4.2	Features of CubeSat platform with 6U	47
4.3	Characteristics of the water propellant	56
4.4	Density and tensile strength of tank material	58
4.5	Typical thermal requirements for spacecraft components. [17]	59

Symbols

c = Effective Exhaust Velocity

I_{sp} = Specific Impulse

I_{tot} = Total Impulse

m_0 = Initial Mass

m_f = Final Mass

m_p = Propellant Mass

m_s = Power Source Mass

m_u = Payload Mass

α = Specific Power Generator Mass

η = Efficiency

β = Technological Level

P_T = Thrust Power

\mathbf{B} = Magnetic Field

\mathbf{E} = Electric Field

Acronyms

EP Electric Propulsion

HET Hall Effect Thruster

GIE Gridded Ion Thruster

PPT Pulsed Plasma Thruster

LEO Low Earth Orbit

MEO Medium Earth Orbit

GEO Geostationary Earth Orbit

S/C Spacecraft

SLS Selective Laser Sintering

SLM Selective Laser Melting

IOD In Orbit Demonstration

IOV In Orbit Validation

COTS Custom off the shelf

Comms Communication System

EPS Electric Power System

OBC On Board Computer

ADCS Attitude Determination and Control System

PPU Power Processing Unit

NSSK North-South Station Keeping

Chapter 1

Introduction

Space flight began with the theoretical studies of Tsiolkosky, Goddard, and Oberth at the beginning of the 20th century. Robert Goddard built the first liquid propellant rocket that broke the sound barrier in 1935. Today, electric propulsion represents the new frontier and solution for many space missions.

The arcjet is an electrothermal thruster that heats the working fluid by means of an electric arc and produces thrust with the conversion of thermal energy into kinetic energy. The evolution of this class of thrusters was born to overcome the limits of resistojets, becoming competitive in space missions that require specific impulses around 600 s and high thrust-to-power ratio. The possibility to choose between different propellants, their geometric simplicity and low weight, compared to electrostatic or electromagnetic thrusters, are the key points that attract the interest of the space market. The goal of this thesis work is to provide the basis for an innovative and competitive project. The first step will be to search for an alternative propellant to those commonly used, such as hydrazine and ammonia, to solve the problems of toxicity and management, in particular a green propellant with low environmental impact that helps to keep the space cleaner and safer. Water reflects these characteristics and shows further advantages. The large availability on Earth, its presence in the form of ice on asteroids which has been detected by recent research and therefore a future possibility of using the resource in-situ, allows cost savings for the entire space mission.

Since the physical phenomena involved in the operation of the arcjet are difficult to understand and require efforts at the initial stages of a new project, an analytical calculation model will be implemented that allows fast but reliable estimates. This analysis will allow the identification of geometric parameters that play a key role in the optimisation of the geometry of the engine for its real performance. The requirement that has been set is to remain in the power class of the order of 1 kW and in this condition the specific impulse and the thrust values will be estimated

based on the selected propellant.

A new technology shall be demonstrated in orbit to be accepted as a new space product, flight heritage is a requirement, in particular when the risk associated with innovation is high. Therefore, the last step of this thesis work will be to define a preliminary design of the space segment for the in-orbit demonstration of the arcjet with a particular focus on the propulsion subsystem and all its components.

Chapter 2

Electric Propulsion and Arcjet

In-space propulsion systems produces thrust that a spacecraft needs to change or maintain its position while performing its mission. Since 1960's various kinds of space propulsion systems have been developing. The common feature of all electric propulsion schemes is the addition of energy to the working fluid from some electrical source. Three main classes of thrusters can be distinguished according to physical phenomena involved:

- *Electrothermal thruster*

The gaseous propellant is heated electrically, and the thrust is generated by thermodynamical expansion of the propellant which occurs within the nozzle. The concept of producing thrust by converting electrical energy into thermal and then kinetic energy has allowed us to overcome the limits of chemical propulsion in which the choice of propellant is essentially based on the chemical energy released by the reaction. Classical electrothermal thrusters are resistojets, in which the propellant is heated by means of an electric resistance through which current flows, and arcjets, in which the propellant is subject to thermal exchanges with an electric arc inside the propellant itself.

- *Electrostatic thrusters*

The acceleration of propellant is due to electrostatic forces. Gridded Ion Thrusters are typical electrostatic device that operate by flowing gas propellant into a discharge chamber where a hollow cathode provides electrons that ionize the gas. The plasma drifts towards the screen grid and the acceleration grid across which a large potential difference is applied in order to accelerate the ions and finally the neutralization of ionic beams is necessary. Hall effect thruster

is essentially a grid-less electrostatic acceleration device in which an applied magnetic field with a primarily radial component is used to trap the electrons in an annular channel leading to a concentrated ionization zone. Thus, an electric field established perpendicular to an applied magnetic field accelerates ions to high exhaust velocities and so this thruster could be considered a hybrid.

- *Electromagnetic thrusters*

These thrusters can be distinguished in stationary and non stationary, but the base concept is the same i.e., a propellant is ionized and the particles are subject to Lorentz forces resulting from the interaction between the current flowing through the plasma and the magnetic field which is either externally applied or induced by the current. The magnetic plasma dynamic thruster is the stationary magnetic thruster, it can be interpreted as a powerful variant of an arcjet in which the arc discharge is of such an intensity that the propellant is ionized to a high degree and accelerated by the electromagnetic fields associated with the discharge. The pulsed plasma thruster is a device of nonstationary electromagnetic propulsion and in this device a discharge ablates and ionizes the surface portion of the solid propellant, creating a propellant plasma which is then accelerated out of the thruster by the Lorentz force.

2.1 Arcjet typical parameters

Arcjet is an electrothermal thruster that uses an electric arc to heat the gaseous propellant whose thermal energy is converted into kinetic energy during expansion in the nozzle. In order to flow an electric current in the propellant it is necessary that inside it there are charges free to move or it must be partially ionized. By immersing two electrodes at a given potential difference in the ionized and globally neutral gas, defined in physics “plasma”, the free charges are set in motion by the electric field effect that is created between the electrodes. The arcjet has an axisymmetric geometry, shown in Fig. 2.1.

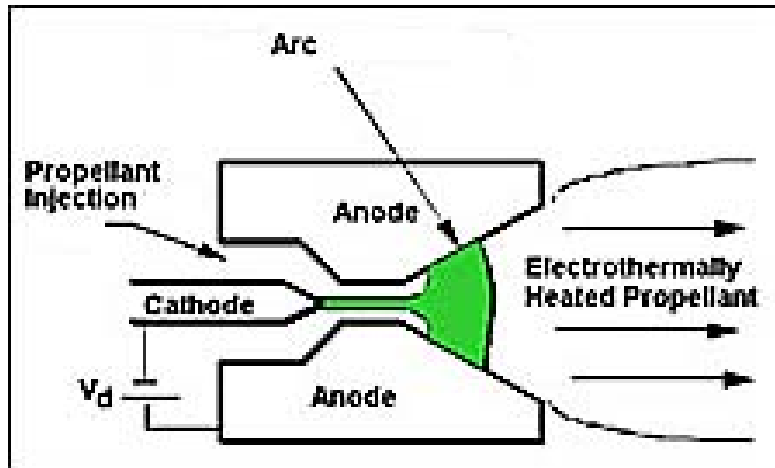


Figure 2.1: Representation of an arcjet system

The cathode is the negative electrode, and it is typically a conical tip rod, the anode is the positive electrode coaxial to the cathode and constitutes the walls of the nozzle in which the propellant gas expands. Under the effect of an appropriate electric field, the electrons move from the cathode towards the anode and by increasing the potential difference they acquire more and more energy until they exceed the first ionization energy which is the minimum required to ionize an atom. As a result of electron-atom collisions, these electrons ionize the propellant in their path, increasing its conductivity. On the other hand, ions from ionization impact the cathode that begins to emit more electrons. The combination of the phenomena due to the presence of the electric field and the ionic bombardment leads to an exponential increase of the current with the consequent ignition of the discharge for a voltage known as Paschen breakdown or Sparking Potential.

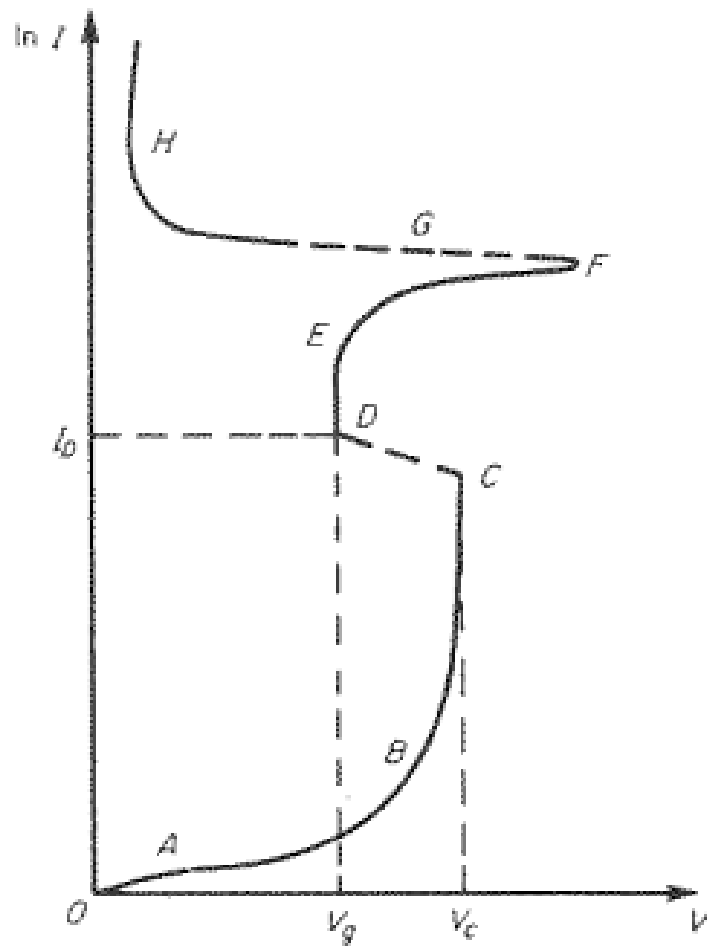


Figure 2.2: Characteristic voltage-current [1]

- In the sections of the curve it occurs that:
- A - B : electrons gain energy greater than ε_i
 - B - C : emission of electrons by ion bombardment
 - C : Sparking Potential
 - D - E : glow discharge
 - E - F : electron emission due to the thermionic effect
 - G - H : electric arc

To stabilize the discharge, it is necessary to abruptly decrease this voltage otherwise the entire system would be destroyed. The glow discharge is supported by the emission of electrons from the cathode by ion bombardment and in this condition the propellant does not reach too high temperatures. However, by

increasing the potential difference, the ions with greater energy bombard and heat the cathode which continues to emit electrons also due to the thermionic effect. Since the current will tend to increase, it will again be necessary to decrease the voltage to support the electric arc. In fact, there are two operating modes of the arcjet thruster which are the so-called high and low voltage modes also characterized by a different position of the electric arc attachment point.

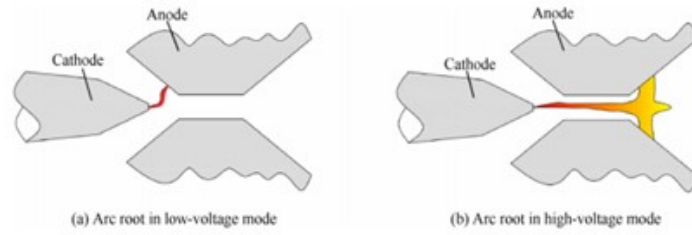


Figure 2.3: Operating modes of the arcjet thruster [2]

In the high voltage mode the arc is dispersed on the surface of the diverging part of the nozzle region where the pressure decreases and the gas flows at high speeds, this means that on the anode walls there is a lower heat flow density and corrosion rate. Conversely, in the low voltage mode, the arc is concentrated in the convergent section of the nozzle, a region characterized by higher pressure and low fluid velocities, which means heat flow density resulting in high corrosion. In its stationary operation the arcjet runs in the high voltage mode, but the ignition process will inevitably lead to high densities of heat fluxes at the anode and this process has a decisive impact on the lifetime of the engine. In stationary operation, the electric arc has a negative current-voltage characteristic because, according to Ohm's laws, if the current increases, so will the number of electron-atom collisions and the conductivity increases much more than the current itself, therefore, to sustain a higher current is sufficient a smaller electric field E or a lower voltage. Due to the Pinch effect, the electric arc can still become unstable even if this effect is appreciable when the thruster works with high currents. In our study it is a negligible phenomenon because our goal is the low power class of the arcjets. To understand this phenomenon, we can refer to an infinitely long electric arc with a given radius through which a current that we suppose of uniform density passes.

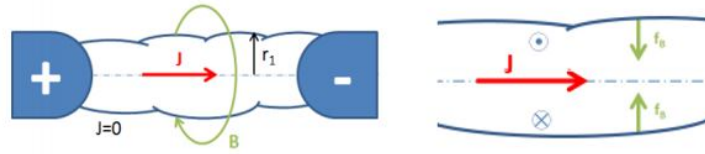


Figure 2.4: Electric arc subject to magnetic forces [1]

The magnetic field lines self-induced by the electric current extend both outside and inside the arc, so from the Ampère-Maxwell equation the trend of the magnetic field can be obtained.

$$\oint_l \mathbf{B} \cdot \mathbf{u} dl = \mu \mathbf{J}_c$$

$$B = \begin{cases} \frac{\mu J r}{2 \pi r_1} = \frac{\mu}{2} j r, & \text{se } r < r_1 \\ \mu \frac{J}{2 \pi r}, & \text{se } r > r_1 \end{cases}$$

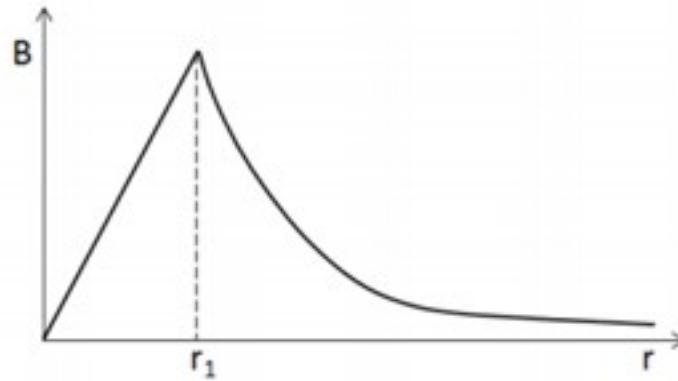


Figure 2.5: Magnetic field across the radial direction [1]

The presence of the magnetic field involves magnetic forces per unit of volume:

$$\mathbf{f}_B = \mathbf{j} \times \mathbf{B} = \begin{cases} \frac{\mu}{2} j^2 r, & r < r_1 \\ 0, & r > r_1 \end{cases}$$

These forces tend to crush the arc on its axis as seen in the figure above. In conditions of equilibrium this effect is balanced by a pressure gradient:

$$-\frac{dp}{dr} = f_B = \frac{\mu j^2}{2} r$$

from which integrating:

$$p - p_{amb} = \frac{\mu J^2}{4\pi} \left[1 - \left(\frac{r}{r_1} \right)^2 \right], \quad p > p_{amb}$$

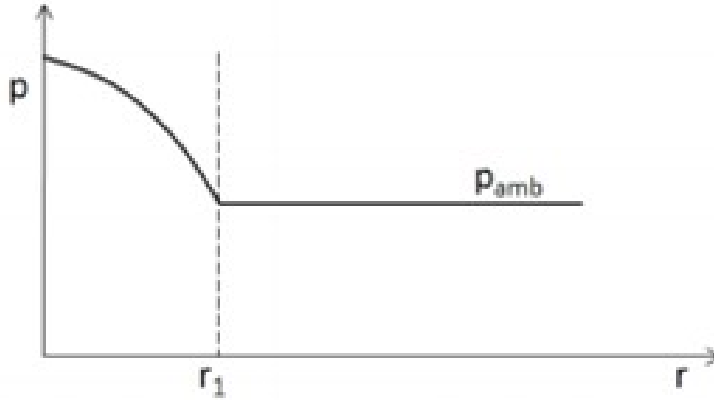


Figure 2.6: Pressure across the radial direction [1]

The parabolic trend of the pressure inside the arc indicates that the pressure is greater along the axis of the engine. This increase which also means higher density and conductivity leads to a non-uniform current density or the arc tends to crush itself on the thruster axis. From this point of view the Pinch effect is positive because it allows the high temperatures of the arc core to be reached without excessively compromising the resistance of the electrode. On the other hand, the Pinch effect must be controlled because it makes the arc intrinsically unstable. There are two types of instability:

- *Sausage instability*, the arc undergoes a symmetrical constriction, in the corresponding region the current density increases, the self-induced magnetic field grows and consequently also the magnetic forces that further compress the arc that will eventually go out;
- *Kink instability*, the arc undergoes asymmetrical constriction, where the magnetic field lines approach the magnetic forces per unit of volume increase as the magnetic field grows and vice versa, so the arc will tend more and more to bend in one direction up to turn off.

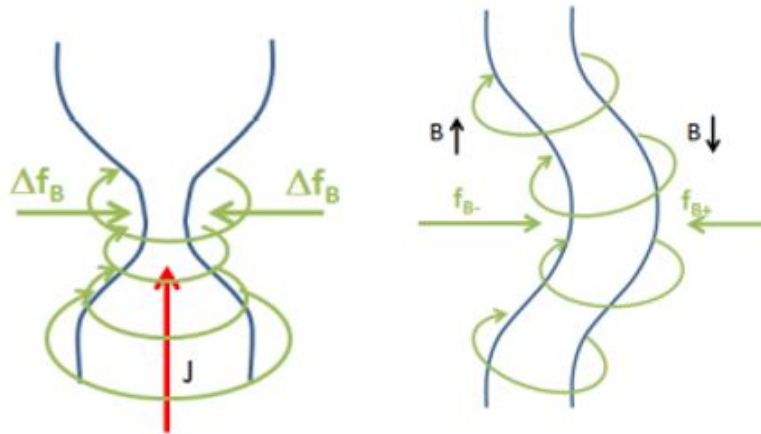


Figure 2.7: Instability of the electric arc [1]

It turns out that the injection of the propellant with a swirl motion or with a tangential velocity component helps not only to counteract the intrinsic instability of the arc but also to improve the effectiveness of heat exchanges. The heat is exchanged by the Joule effect, deposited in the electric arc and transmitted to the surrounding propellant which by conduction heats all the propulsive fluid. The cathode is heated by radiation from the electric arc and ion bombardment while the propellant introduced from the bottom of the chamber with a swirl motion and the emission of electrons contribute to its cooling. In turn, the anode is also heated by radiation from the electric arc and electrons that hit the electrode and cools by giving heat to the propellant and radiating outwards. Near of the anode and cathode surface we see an excess of negative and positive charges respectively due to the effect of the charge shielding while in the central area the fluid is essentially a globally neutral plasma. Thus, the voltage profile between the electrodes is characterized by rapid growth near the cathode, or fall at the cathode, from a relatively uniform central voltage region known as the thermal column, and another rapid growth near the anode, or fall region at the anode; the trend of the electric field \mathbf{E} will be constant in the plasma area and characterized by two peaks at the electrodes; this phenomenon can be seen in Fig. 2.8. The central column which occupies the interval between the two electrode-fall regions is a plasma consisting of a mixture of electrons, ions and neutral atoms at nearly the same temperature which about $10^4 K$. The random thermal velocities of the electrons far exceed their mean drift speeds since the electric field is weak in this area the predominant ionization mechanisms are thermal electron collisions and photoionization. The cathode and anode falls are typically less than $20V$, they have the same spatial extension and in both these regions the electrons, in contrast to central column,

are accelerated by the strong electric field.

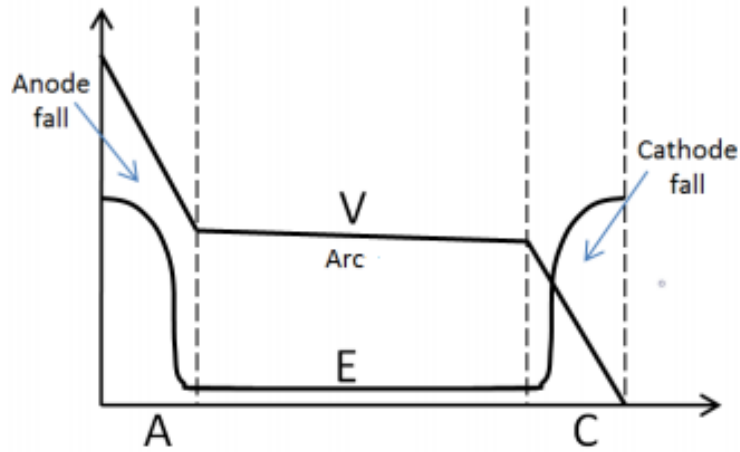


Figure 2.8: Voltage and electric field between the electrodes [1]

As a first approximation, the performance of an arcjet can be evaluated starting from the power balance:

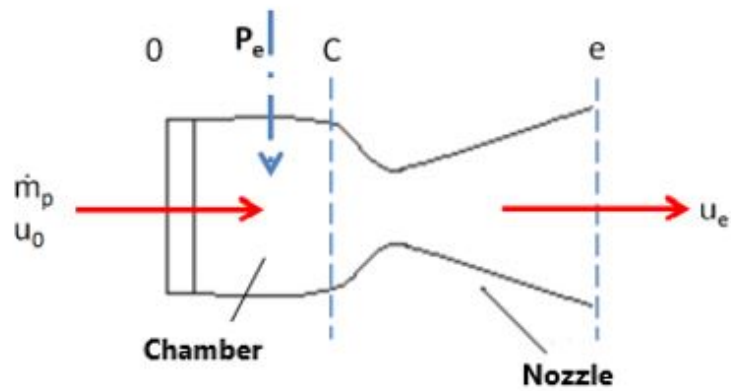


Figure 2.9: A generic electric thruster [1]

$$P_e = \dot{m}_p (h_c^\circ - h_0^\circ)$$

$$P_e = \dot{m}_p \left(\frac{u_c^2}{2} + h_c - \frac{u_0^2}{2} - h_0 \right)$$

The initial speed u_0 and enthalpy h_0 are those of the tank where the propellant is stationary and stored at low temperatures, since even the speed in the chamber u_c is still low all these terms can be neglected with respect to the high static enthalpy of the propellant in the chamber h_c , so simplifying:

$$P_e \approx \dot{m}_p h_c = \dot{m}_p c_p T_c$$

In the energy balance per unit of time between the heating chamber and the outlet section we can again neglect u_c and also the static enthalpy in the outlet section h_e as the vacuum temperature is very low. We can write:

$$0 = \dot{m}_p (h_e^\circ - h_c^\circ)$$

$$0 \approx \dot{m}_p \left(\frac{u_e^2}{2} - h_c \right)$$

Then, the ideal effective exhaust speed is:

$$u_{e,id} \approx \sqrt{2h_c} = \sqrt{\frac{2P_e}{\dot{m}_p}} = \sqrt{2c_p T_c}$$

or

$$u_{e,id} \approx \sqrt{2 \frac{\gamma}{\gamma - 1} \frac{R^*}{\mathcal{M}} T_c}$$

This speed is limited by the maximum temperature that can be reached, by the molecular weight of the propellant used and by the electric power available. Although higher temperatures can be reached in arcjets than in resistojet, the specific impulse values related to the effective exhaust speed through gravitational acceleration g are limited. There is the presence of losses classified as follows:

- *Thermal losses*

$$\eta_{th} = \frac{P_{thrust}}{P_e}$$

take into account the dispersed heat because not all the electrical power supplied is converted into thermal power to be transferred to the propellant;

- *Aerodynamic losses*

$$\eta_{ae} = \frac{T_c/2}{1/2\dot{m}_p u_e^2} = \frac{1/2\dot{m}_p c^2}{1/2\dot{m}_p u_e^2} = \left(\frac{c}{u_e} \right)^2$$

due to non-homogeneous heating of the flow, the boundary layer and the divergent component of the flow in the exit section of the nozzle;

- *Frozen flow losses*

$$\eta_{ff} = \frac{u_e^2/2}{h_c} = \frac{h_c - h_e}{h_c} = \left(\frac{u_e}{u_{e,id}} \right)^2$$

take into account the part of energy expended in the phenomena of dissociation and ionization and which is not recovered because the chemical equilibrium is not reached in the nozzle.

The latter predominate in the arcjets and the way to counter them is the increase in pressure which plays against the phenomena of dissociation. Increasing the pressure also means increasing the density of the propellant in the chamber, improving the effectiveness of heat exchanges, but also affects the characteristics of the electric arc.

2.2 Arcjet application and maneuver

The extremely high thrusts and low specific impulses characterizing the chemical propulsion on the one hand and high specific impulses and low thrusts provided by the electrostatic propulsion on the other hand, make electrothermal thrusters good candidates in missions with power and / or time requirements. Theoretically, a lower consumption of propellant is obtained by increasing the specific impulse, but this increase is linked to a greater electrical power available which involves an increase in the specific mass of the power generator and thus in the total mass. Solving the payload optimization problem allows to obtain the optimal specific impulse for a mission and therefore to understand which is the most suitable propulsion system. We divide the initial mass of the system into the payload mass m_u which contains the mass of the structures and payload, power generator mass m_s and propellant mass m_p :

$$m_0 = m_u + m_s + m_p$$

If at the end of the mission all the propellant has been consumed, the final mass will be the sum of the masses of the payload and of the generator, therefore the initial mass can be expressed as the sum of the final and propellant masses:

$$m_f = m_u + m_s$$

$$m_0 = m_f + m_p$$

Therefore, we can define the payload fraction:

$$\frac{m_u}{m_0} = \frac{m_f}{m_0} - \frac{m_s}{m_0}$$

The rocket equation links the initial mass to the final mass with the effective exhaust velocity and Δv values:

$$\Delta v = c \ln \left(\frac{m_0}{m_f} \right)$$

or

$$m_f = m_0 \exp \frac{-\Delta v}{c}$$

Then the mass of the generator can be considered proportional to the power delivered by it through the specific mass α and so:

$$m_s = \frac{\alpha}{2\eta} T c = \frac{\alpha}{2\eta} \dot{m}_p c^2$$

with the appropriate substitution, the expression of the payload fraction is obtained as a function of the parameters $c/\Delta v$ and Δt :

$$\frac{m_u}{m_0} = e^{-\frac{\Delta v}{c}} - \frac{\alpha}{2\eta} \frac{(1 - e^{-\frac{\Delta v}{c}})}{\Delta t} \left(\frac{c}{\Delta v} \right)^2 \Delta v^2$$

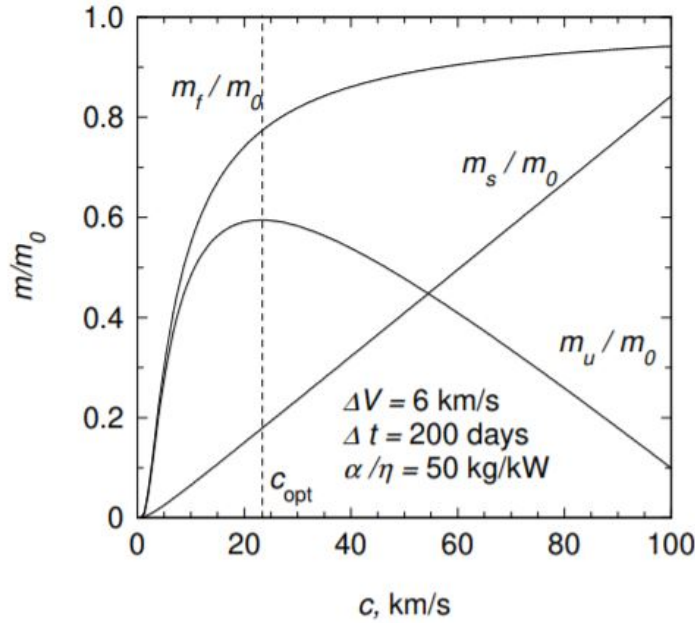


Figure 2.10: Optimal specific impulse [3]

It appears that the optimal specific impulse increases if the required Δv of the mission is higher while for the same Δv , if the mission does not require relatively short times, the necessary thrust decreases and consequently also the required electrical power or the specific mass of the generator power in favour of specific impulse and mass savings. Arcjets can provide specific impulse values from 400 to 2000 s depending not only on the available power but also on other factors such as the propellant used. The wide range of specific impulse values makes these electrothermal devices suitable for different purposes. The small satellites that have a total mass from 100 to 500 kg and especially the CubeSats whose mass is a few kg have revolutionized the observation of the Earth and space with a considerable reduction in costs since the mid-90s.

Their use has led to the development of arcjets with powers in the order of hundreds of Watts as on the one hand a greater power implies larger solar panels that exceed the budget imposed by these satellites and on the other hand the use of batteries for operation cyclical thruster causes a mass problem and greater electrode erosion than continuous operation. For example, a generic mission of a small satellite with a wet mass of 200 kg and the Δv requirement of about 200 m/s can be accomplished with a propulsion system with a power of 200 W and a mass of less than 20 kg and so 10% of the total mass reaching 400 s specific impulse with only 10 kg of propellant leaving 10 kg for the total mass of the propulsion system or additional payload. With an estimate of the dry mass of the propulsion system at 6 kg (0.3 kg for the propeller, 1 kg for the PPU, 1.5 kg for the propellant fuel system and an additional 3 kg for mounting and tank) the required Δv can be obtained. Much research is aimed at engines in the kW power class. They are suitable for attitude control and NSSK (North South Station Keeping) missions of satellites in GEO orbit. For this purpose, the engines must be turned on once a week when the power is deallocated from the communication payloads to the propulsion system for manoeuvres of 30-90 minutes. An electrostatic thruster that provides relatively lower thrusts should run for more than 5 hours a day and since it is not possible to deallocate the power from the payload for such a long time in this case it would be necessary to have higher power levels. The electrothermal devices are used in lifting the orbit as needed by the satellites of the navigation constellations. These satellites typically of masses around 700 kg have an available power of 1 kW and must be brought to MEO by LEO within a year.

If the arcjet proves to have a lifetime of this order with continuous operation, it could replace Hall Effect thrusters or gridded ion thrusters that require higher powers to perform the mission at the same time and are much more complex and heavier.

To limit the impact of space debris, the European Code of Conduct requires a maximum time in orbit of 25 years after the end of the satellite service. An

	Resistojet	Arcjet	GIE	HET/HEMPT	PPT	MPDT/ECR
Type	Electrothermal	Electrothermal	Electrostatic	Electrostatic	Electromagnetic	Electromagnetic
Achievable thrust (mN)	0.5–6000	50–6800	0.01–750	0.01–2000	0.05–10	0.001–2000
Isp (s)	150–850	130–2200	1 500–10 000	600–3000	1400–2700	200–3200
Efficiency η_e (%)	30–110 ^{a)}	25–60	30–90	20–70	5–30	20–70 ^{b)}
Thrust-to-power ratio (mN/kW)	450–700	150–600	20–250	150–300	50–200	150–500
Operational time	Month	Month	Years	Month	Years	Weeks
Propellants	NH ₃ , hydrazine, H ₂ , Xe, and N ₂	H ₂ , N ₂ , hydrazine, and NH ₃	Xe, Kr, Ar, Bi, I ₂ , and H ₂ O	Xe, Kr, Ar, and I ₂	PTFE	Ar, Xe, H ₂ , and Li
Benefit	Low level of complexity	High thrust	High Isp and high efficiency	High power-to-thrust-ratio	Simple device and solid propellant	High Isp and high thrust density
Drawback	Very low Isp	Low efficiency	Low thrust density and complex PPU	High beam divergence and channel erosion	Low efficiency	Low lifetime and high power requirement

Table 2.1: Characteristic of main EP thruster types [4]

active propulsion system is necessary to ensure correct positioning in orbit and the required propellant and the mass of the propulsion system should be minimal to be economically advantageous, therefore the arcjet is to be considered among the best candidates to perform this task as it shows their use in ESA’s Clean Space project. A further mission concept would be the continuous compensation of the atmospheric drag of the satellites in LEO and the International Space Station. If the compensation requirements are $0.3mN/m^2$ in an orbit of $400km$ and up to $15mN/m^2$ in an orbit of $200km$, an arcjet with about $30mN$ of thrust can compensate for the atmospheric drag of a small satellite of $2m^2$ cross section at $200km$ high or a $100m^2$ station at $400km$ high . Last but not least is the primary propulsion role that the arcjet can play in some phases of interplanetary missions. For example, the thrust of about $100mN$ provided by such a thruster is suitable in the early stages of a mission to the Moon, wanting to minimize the time that the satellite spends to cross the Van-Allen belts and reduce possible radiation damage to the solar panels and the electronics on board the satellite.

2.3 Propulsion strategy: Comparison with similar thruster

The arcjet, and electrothermal propulsion in general, is based on the electric heating of the propellant which is then expanded in the De-Laval nozzle. Chemical propulsion, on the other hand, involves a combustion reaction typically between an oxidant and a fuel to produce thrust. To understand the limits of chemical

propulsion compared to electric propulsion, we can still consider the power balance between the inlet, combustion chamber and output sections of the engine:

$$\dot{m}_p (h_c^\circ - h_0^\circ) = \dot{m}_p E_{ch}$$

$$\dot{m}_p h_e^\circ = \dot{m}_p h_c^\circ$$

As a first approximation, the input and chamber speed and the initial enthalpy of the propellant can be considered negligible compared to the energy developed in the chamber; therefore, the effective exhaust speed can be obtained from the power balance:

$$u_e \approx \sqrt{2E_{ch}} = \sqrt{2h_c} = \sqrt{2c_p T_c}$$

From the equation it can be seen that the effective exhaust speed and therefore the specific impulse linked to it is limited by the chemical energy per unit of mass developed during the reaction within the propellant.

On the other hand, the specific impulse in electric propulsion is a function of the available electric power:

$$\dot{m}_p \frac{u_e^2}{2} = \eta P_e$$

$$u_e = \sqrt{\frac{2\eta P_e}{\dot{m}_p}}$$

Therefore, it allows to overcome the upper limit of specific impulse that can be reached with the chemical propulsion and to minimize the amount of propellant. However, with electric propulsion alone it would not be possible to overcome the gravitational attraction of the Earth since the accelerations provided are typically one hundredth of the acceleration of gravity, therefore its use is limited to when the satellite is already in orbit and the force of gravity it is balanced by the centrifugal force acting on the orbit. Typical Δv values required in space missions are shown in the following table:

Table 2.2: Typical Δv value required in space missions [3]

Mission	Δv [km/s]
LEO insertion	10
1 year station keeping	0.5
LEO-GEO impulsive	3.5
LEO-GEO spiral	6
Earth escape impulsive	3.2
Earth escape spiral	8

Recalling the Tsiolkovsky equation:

$$m_f = m_0 e^{-\frac{\Delta v}{c}}$$

it can be deduced that for a given Δv if the specific impulse is small, as happens in chemical propulsion, the final mass tends to decrease to the point of making the mission impossible. The small accelerations provided by electric propulsion translate into longer thrust times and if these are acceptable the advantages of electric propulsion are relevant. If you think of a mission in which the required Δv is $6km/s$, the same payload fraction could be brought to its destination with electric propulsion, accepting longer times than a chemical engine that uses the LOX / LH2 mixture with the highest specific impulse value among the propellants used in the order of $450s$, but with a significant cost reduction. Compared to chemical propulsion, electric propulsion allows:

- Possibility of carrying greater loads even if in longer times, given the low thrust / weight values;
- Thrust adjustment;
- Availability of electric power once the mission is completed

In the subclass of resistojet devices, the temperature of the chamber is necessarily limited by the materials of the walls and/or of the heater coils to around $3000K$ or less, consequently the exhaust speeds cannot exceed $10000m/s$ which is in any case a value double that of chemical rockets. Beyond the losses due to frozen flows, the main challenge in the design of a resistojet is to maintain integrity at high temperatures by trying to reduce viscous and radiative losses that affect the efficiency of the engine. A typical resistojet operating at a power level of $750W$ reaches a exhaust speed of $3500m/s$ or a specific impulse of about $350s$ and a

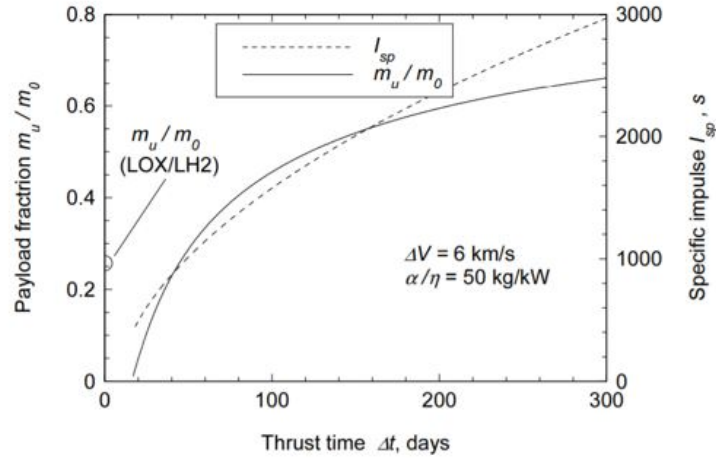


Figure 2.11: Performance comparison of chemical thruster and EP [3]

thrust of $0.3N$ with an efficiency of 80%. Their attraction can be mainly in the prompt integration with storage and propellant management systems previously developed and used for monopropellant thrusters. Furthermore, as they require low operating voltages they do not require complex power processing units. However, there remains a limit to the specific impulse due to the temperature value which must be compatible with the resistance of the materials. To overcome the problem by always adopting the same principle of thrust generation by electric heating of the propellant, the arcjets introduce an electric arc in the central area of the engine in order to create temperature gradients that allow the achievement of much higher temperatures along the axis of the thruster and lower temperatures near the walls of the chamber and of the nozzle so as not to compromise their integrity. This allows to reach a higher specific impulse while decreasing efficiency since part of the thermal energy is spent in dissociation and ionization phenomena of the propellant and no longer recovered, that is losses due to frozen flow predominate as already mentioned in the previous paragraphs. They generally operate at higher voltages than the spacecraft bus voltages and therefore require dedicated power processing units whose mass of the order of 2.5kg/kW is greater than engine itself, that is lightweight and compact. Finally, despite the management of the electrodes corrosion problem that must be considered in the design of these devices, the operating life is about double that of a resistojet.

Chapter 3

Arcjet detailed description

3.1 Propellant analysis

The choice of propellant is often driven by several factors in conflict with each other so a compromise must be found according to requirements and expected performance. As mentioned in the previous paragraphs, it is known that in electric propulsion the use of low molecular weight propellants allows to reach a higher specific impulse value. This value improves for species exhibiting fast internal modes that maximize specific heat capacity. On the other hand, the high temperatures support the ionization and dissociation processes thus it is necessary to know the electrical and thermochemical behaviour of the species. A good level of ionization and electrical conductivity allows the establishment of the electric arc used as means of heating in the arcjet, but a lack of chemical equilibrium in the outlet section nozzle as a result of the dissociation of the species involves an amount of energy which remains frozen in the propellant or frozen flow losses that affect the specific impulse that can be reached. Furthermore, in a device in which the electrodes are in direct contact with the propellant gas, it is necessary to know the erosion extent of the critical components that limits the life of the thruster itself, so it will be necessary to evaluate the chemical compatibility between the materials and species. A higher specific impulse is expected from a low molecular weight propellant gas than a higher molecular weight one, but it may happen that the losses due to frozen flow or the costs related to storage in space have a greater weight such that the best choice is not always the lightest propellant.

The emblematic example is H_2 which has high specific heat and electrical conductivity to the point that assuming a chamber heating temperature of about $3000K$ would be reached, ideally, a specific impulse would be obtained around $1100s$.

The Fig.3.2 shows that the frozen flow efficiency is low when the pressure value

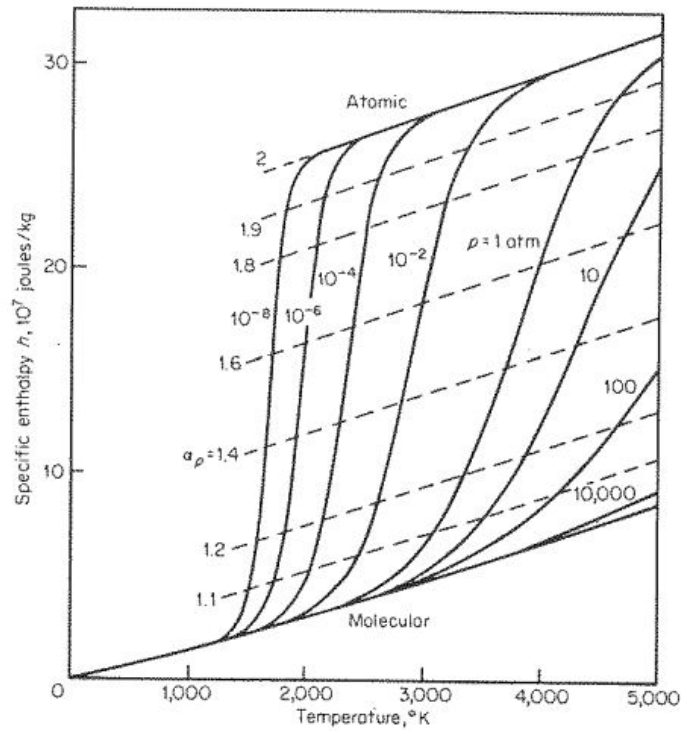


Figure 3.1: The effect of dissociation on the enthalpy of hydrogen [5]

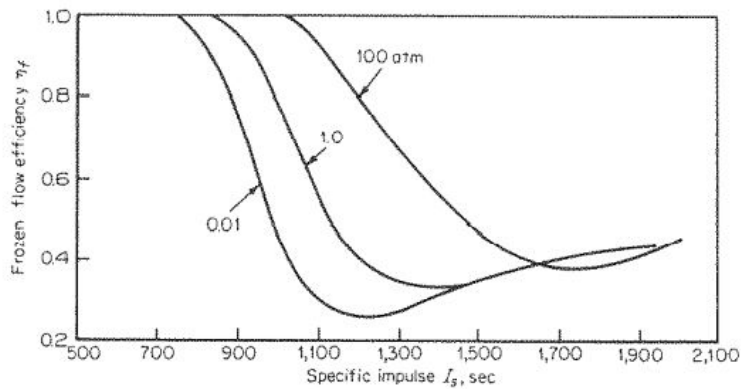


Figure 3.2: Theoretical variation of frozen flow efficiency with specific impulse for Hydrogen at various pressures [5]

is moderate and if we add to these losses the aerodynamic and thermal ones, the specific impulse decreases further to the point that it is not possible to exceed the value of 600 s. Thus, One way to counteract frozen flow losses is to act on the

pressure in the chamber.

The Saha equation following describes the percentage of ionized atoms or ionization degree α in a gas in thermal equilibrium:

$$\frac{\alpha^2}{1 - \alpha^2} = 2 \frac{(2\pi m_e)^{3/2}}{ph^3} \frac{f_{iA}}{f_{i+}} e^{\frac{\epsilon_i}{k_B T}}$$

Here m_e is the mass of an electron, k_B is the Boltzmann constant, ϵ_i is the energy required to remove i electrons from a neutral atom, f_{iA} and f_{i+} are the partition functions of the atoms and ions, respectively. Therefore the temperature favors the ionization of the gas while the pressure opposes it so one way to limit frozen flow losses is to increase the pressure. Let us recall the expressions of the electric power and the flow rate:

$$P_e = \frac{\dot{m}_p c^2}{\eta} \frac{1}{2}$$

$$\dot{m}_p = \frac{p_c A_t}{\sqrt{\mathcal{R}T_c}} \Gamma$$

The latter allow us to understand that the increase in pressure in the chamber involves an increase in flow rate and the electric power value of a few kW that we have set will heat a greater flow rate, this means that the gas temperature and the specific impulse decrease. Consequently, the pressure cannot rise arbitrarily and frozen flow losses cannot be eliminated.

In the use of hydrogen there is also the further problem of storage since liquid hydrogen requires cryogenic storage at about 20 K and the tanks must be well insulated to avoid its boiling. The high losses and the high operating costs of this chemical element do not make it a good candidate not only for the operation of the low power arcjets but in general for electrothermal propulsion.

Helium is the second lightest element after hydrogen with respect to which it has the great advantage of a high first ionization energy, about 24.46 eV, which means negligible frozen flow losses but its liquefaction temperature, about 4 K and so lower than that of hydrogen, it is limiting in its effective use in space due to the insurmountable problems of storage.

Ammonia, on the other hand, does not require refrigeration for its liquid phase and once heated the heavy molecules dissociate into low molecular mass constituents introducing frozen flow losses.

Similarly, hydrazine is easily storable and allows to reach high performances thanks to the exothermic dissociation reaction which increases the enthalpy of the

propellant with a lower electrical input even if at the same time the problems of heat exchange in the chamber and on nozzle wall increase with the relative increase in erosion of the materials. Its current use is avoided due to its toxicity which involves many dangers and increases the test phases costs and times.

We remember that the specific impulse is:

$$I_{sp} = \frac{I_{TOT}}{m_p g_0}$$

where

$$I_{TOT} = T \Delta t$$

and the mass propellant m_p :

$$m_p = \int_{t_0}^{t_f} \dot{m}_p dt$$

If the thrust T and the flow rate \dot{m}_p are constant in time Δt we can write:

$$I_{sp} = \frac{T \Delta t}{\dot{m}_p \Delta t g_0} = \frac{u_e}{g_0}$$

From the inversion of the expression we obtain u_e which we replace in the energy balance between the heating chamber and the outlet section of the nozzle, with the simplifications already clarified in the previous chapter, and we obtain the static enthalpy value that we expect the gas to have in the chamber to obtain the preset specific impulse.

Thus:

$$\frac{1}{2} u_e^2 = \frac{1}{2} u_c^2 + c_p (T_c - T_e) \approx c_p T_c = h_c$$

$$h_c \approx \frac{(I_{sp} g_0)^2}{2}$$

Assuming that our goal is to reach a specific impulse of 600s, certainly an optimistic value but it is good to be conservative, it is evaluated by above equation the enthalpy in the chamber, knowing the trend of the c_p as a function of temperature, from the product of these two quantities it is possible to evaluate the enthalpy of the gas for different temperatures which is compared with the expected value for that specific impulse. In this way it is possible to trace the temperature value that must be reached in the chamber for the different propellants.

The constant pressure specific heat c_p of the propellant gas per unit of mass limits the specific impulse obtainable by defining the maximum enthalpy that can

be imparted to a gas at a given temperature. Polynomial expressions of c_p as a function of temperature and coefficient values were searched in the databases of the NIST (National Institute of Standards and Technology) Chemistry WebBook. For any gaseous species, the expression of specific heat at constant pressure are in the following form:

$$c_p = A + Bt + Ct^2 + Dt^3 + E/t^2$$

where A, B, C, D and E are the constants, t is the temperature in K divided 1000 as NIST establishes.

The c_p values of the previously mentioned chemical elements, namely hydrazine, ammonia, helium and hydrogen, are compared with each other together with other species such as argon to highlight the different behaviour of the possible propellants. In the following graph in Fig. 3.3 we see that H_2 has the highest specific heat capacity value, followed by NH_3 , He , N_2H_4 and while allowing to reach excellent specific impulse values with tolerable temperatures in the heating chamber by materials of the anode and cathode, as the Fig. 3.4 shows, they have problems of frozen flow losses and too high costs related to their storage as discussed above.

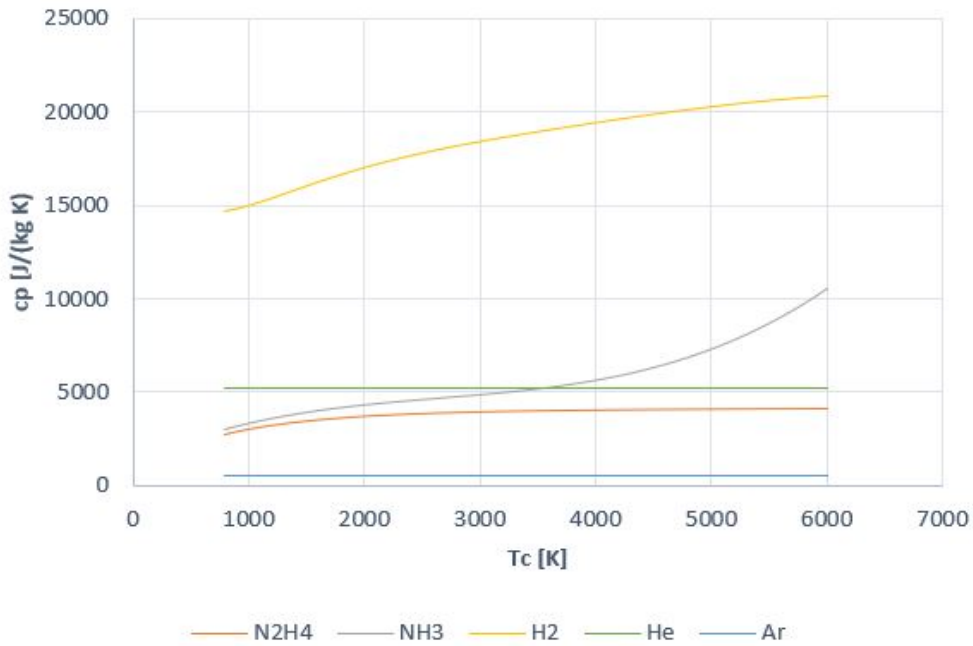


Figure 3.3: Variation of specific heat at constant pressure with temperature for hydrogen, ammonia, helium, hydrazine, argon

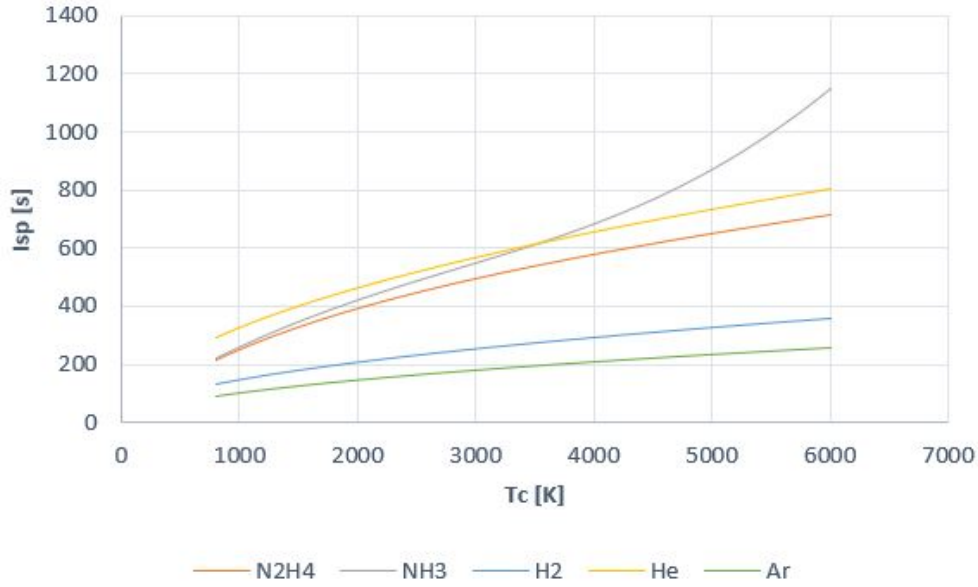


Figure 3.4: Variation of specific impulse with chamber temperature for hydrogen, ammonia, helium, hydrazine, argon

Conversely, *Ar* is characterized by a relatively lower c_p such that it is to be excluded in the design of a low-power arcjet which requires a specific pulse value of at least 500s. If a specific impulse of less than 300s were accepted, the expected temperature in the chamber would drop below 6000K and the thermal loads would still be too high, so *Ar* is certainly an unsuitable propellant. NH_3 has a molecular weight of $17.03g/mol$, lower than hydrazine with $32.04g/mol$, and at the same temperature of the gas in the heating chamber the specific impulse obtainable with ammonia is greater. In the absence of losses, to obtain a specific impulse of about 600s, the temperature in the heating chamber that is expected with hydrazine is around 4200K while with ammonia 3300K. These are ideal values, i.e., in this preliminary phase the aerodynamic, thermal and frozen flow losses were neglected but the general behaviour deduced from research based on previous projects is known.

Since the purpose of the study is to create a competitive project, in addition to the typical propellants used in electrothermal propulsion, other gaseous species have been analyzed. As expected, Xenon is not suitable in this propulsion technology having a very high molecular mass, $131.293g/mol$, and therefore a low c_p , the temperature to which the gas should be brought would be too high and far above the limits imposed by the resistance of the materials used for the walls of the engine. Among the alternative propellants for the electric propulsion, hydrogen peroxide H_2O_2 seemed attractive for its molecular weight, $34.0147g/mol$, very

close to that of hydrazine and in fact the calculation procedure described above led to a temperature value in the heating chamber of the order of $3400K$ comparable with the the chamber temperature measured on a typical thermal profile of the state-of-the-art arcjet of the same power class powered by hydrazine as shown in Fig. 3.5 .

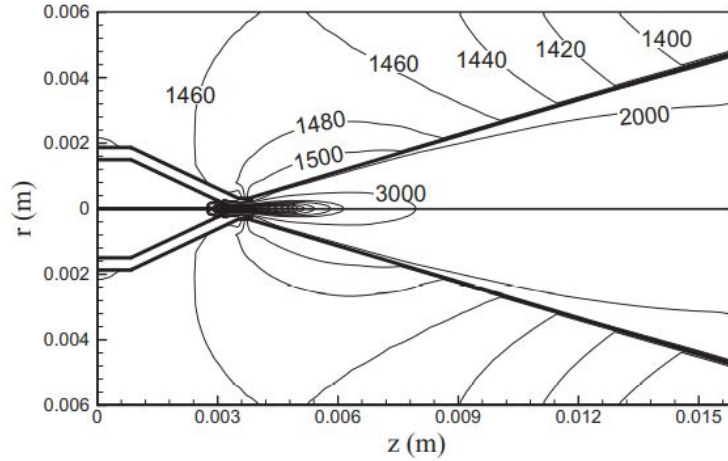


Figure 3.5: Computed isotherms within the gas region and the solid region [6]

Now, the trade-off between desired performance, development costs, management and safety has led to the idea of analyzing water as a possible propellant. By reducing the specific impulse target value to $450s$, according to the calculations, the temperature value in the chamber results around $3000K$. H_2O which could ideally guarantee acceptable performance with obvious advantages. It is a green, reusable, ecological propellant and can make the space cleaner and safer. Space exploration has shown the presence of water/ice on the surface or inside asteroids, the Moon and Mars so it may no longer be necessary to bring all the propellant that is needed from Earth. The use of in-situ resources makes it possible to drastically reduce costs, but it is necessary to develop a specific technology. Recent research has focused on water propelled arcjets but the need for a gas generator for the vaporization of the fluid and the consistent erosion of the electrodes slow down its development.

Based on these considerations and from the perspective of an innovative project of a low-power arcjet that is competitive in the current market, water is the selected propellant to feed the electrothermal device of this study.

3.2 Electrode and material

The working structures of the thruster must be made of materials that have specific characteristics. The electrodes are essentially composed of a good conductor and an electrical insulator will be required between the surfaces of the cathode and the anode.

The metal used for the latter is to be selected according to needs. It must exhibit a high thermal conductivity to be able to remove thermal loads especially in the arc attachment regions, this conductivity must also be maintained as the temperature increases. Thermal loads are a critical point in the operation of the arcjet which can compromise the structural strength of the components; therefore, good mechanical properties are required of the selected material even at high temperatures. To cope with ionic bombardment the cathode must be resistant to sputtering. Furthermore, the melting point must be as high as possible in order to have a greater margin of thermal energy that can be supplied to the propellant and gain in terms of performance. Among the parameters to be considered there is also the work function or the minimum energy required to be able to tear an electron from the metal, clearly a lower work function results in less heating and, hence, reduced wear on the electrodes. If the engine is cooled radiatively it is good that it behaves like a black body with high emissivity. Finally, the manufacturing of the material itself must be considered.

For the insulators the requirements are similar except for some of them: clearly the insulator will not be subject to ionic bombardment so it will not have to show resistance to sputtering as well as no thermionic emission is required. However it must withstand high temperatures and therefore have good conductivity and a high melting point.

As regards the conductive material, most metals are able to provide an adequate conductivity value so that the melting point and thermal conductivity, especially at high temperatures, become discriminating parameters for selecting the material. Some metals are analyzed and their characteristics are tabulated in Tab. 3.1 below.

Tungsten has the highest melting temperature, in fact most of the state-of-the-art

Metal	Density /Kg m ⁻³	Melting point /K	Thermal Conductivity ($Wm^{-1}K^{-1}$) at various temperatures(K)											
			100	200	400	600	800	1000	1200	1500	2000	2500		
Iridium	22500	2720	172	153	144	138	132	126	120	111				
Molybdenum	10240	2894	179	143	134	126	118	112	105	98	90	86		
Niobium	8570	2741	55.2	52.6	55.2	58.2	61.3	64.4	67.5	72.1	79.1			
Tantalum	16600	3269	59.2	57.5	57.8	58.6	59.4	60.2	61.0	62.2	64.1	65.6		
Tungsten	19300	3660	208	186	159	137	125	118	113	107	100	95		

Table 3.1: Characteristics of various metals [7]

arcjets that have been studied for our work employ this metal for the anode and cathode structures, it seems the most appropriate choice.

Additive manufacturing allows the creation of components of almost arbitrary complexity without additional costs or times and can be exploited in space. In these applications, the methods that can be used are Selective Laser Sintering (SLS) and Selective Laser Melting (SLM) as they allow to process metals commonly used in the sector. Their basic concept is the same, that is to locally heat a bed of powder with a localized laser beam and a continuation of the solidification of the treated part continue with the drafting of a subsequent layer of metal powder. The difference between the two technologies is in the power of the electron beam: in the SLM the laser locally melts the layer of dust creating a real pool of fusion while in the SLS the powers involved are lower. The SLM allows to treat materials with a high melting point, such as tungsten, even with excellent levels of density. It is true that excellent precision is not achieved with this technology, but if the aim is to create integrated regenerative cooling channels in which dimensional tolerances are not necessary, then the arcjet nozzle could be an excellent candidate [8].

Insulators are generally ceramic or plastic materials whose resistivity decreases rapidly with the increase in temperature. However, plastic materials are to be excluded because they are characterized by a low melting temperature. The critical point of the insulating layer is the strong temperature gradient which can cause it to break. Other parameters discriminating the choice of material in this case are electrical resistance and thermal conductivity; these characteristics are shown in Fig. 3.6 and in Fig. 3.7 for various insulators. As you can see, there is not much difference between Boron Nitride BN and Beryllium Oxide BeO which show the best thermal conductivity in the wide temperature range. However, for the BN the trend is almost constant and at temperatures above 1000 K its performance is better than the BeO, as well as being lighter, relatively inexpensive and easily machined.

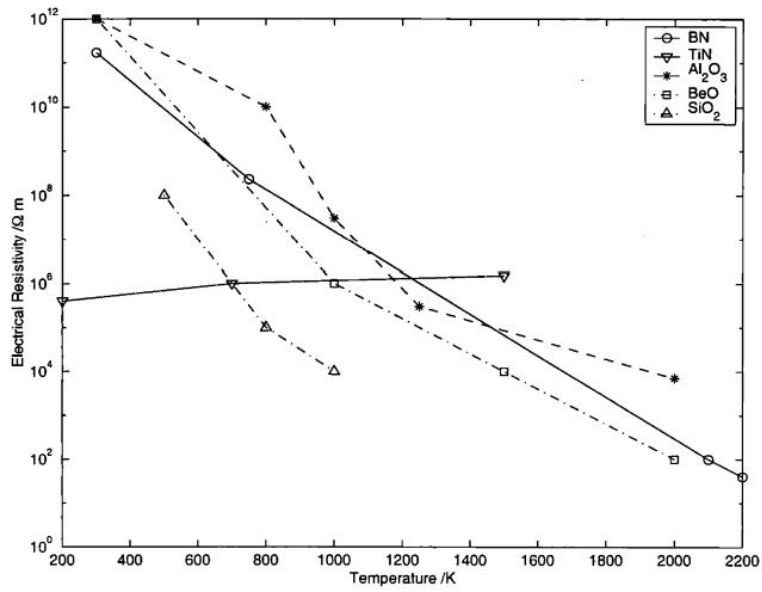


Figure 3.6: Electrical resistivity of ceramic materials [7]

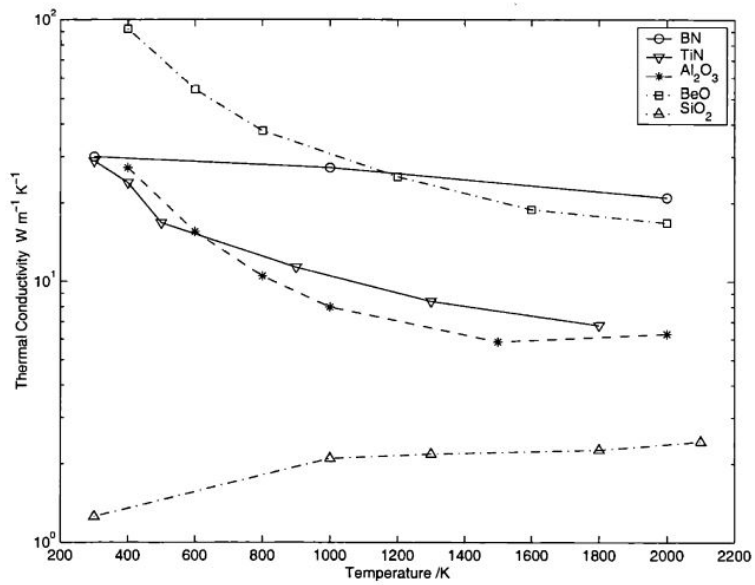


Figure 3.7: Thermal conductivity of ceramic materials [7]

3.3 Adopted model description

The design of an arcjet thruster and the estimation of its performance may require very long calculation times using appropriately developed numerical codes although these allow to detect some physical effects at the base of phenomena involved. In a preliminary phase in which not many data is available other than those based on previous work, it becomes reasonable to adopt a simplified model to predict performance in a simple and fast way. The model adopted is based on a 1D analysis, it will not be numerically accurate but preserves physical consistency and constitutes a starting point for subsequent optimizations by providing orders of magnitude of the input parameters. Typically, in the operation of the arcjet an electric arc develops from the cathode towards the output section of the constrictor along the axis of the engine while the propellant, injected upstream of the negative electrode, is heated by the arc itself and expands in the nozzle . It has been noted that the arc acts as a partial fluidynamic plug on the flow so that the effective flow area comes from the difference in the cross section of the constrictor and the arc cross section appropriately defined. Therefore the first assumption is to consider the flow divided into two regions, so a "*Dual Channel Model*" [9] will emerge:

- *Inner stream* or *Arc column*, central area where the arc develops;
- *Outer stream*, flow area surrounding the electric arc.

It is assumed that the outer flow evolves isentropically, the gas in direct contact with the arc reaches a temperature such as to become partially ionized and electrically conductive or, in other words, it becomes part of the arc itself that swells towards the section of exit of the constrictor. The arc growth is to be understood as a result of radial diffusion of the ohmic heat into the surrounding external gas. This implies that the length and diameter of the constrictor must be designed so that the arc is as close as thermally permissible to the walls of the constrictor. It is important to emphasize that in order to predict performance, the conditions within the arc itself, i.e. dissociation, ionization, gas in non-equilibrium conditions, are quite irrelevant in this regard as long as it is possible to calculate the arc radius. This explains the success of such an analysis model in the preliminary design phase.

We call R_a the external radius of the electric arc and R the constrictor radius as shown in figure below: Therefore, the inner flow region develops axially along x with $0 < r < R_a$ and inside it the temperature will be in the ionization range of the propellant being this electrically conductive, vice versa the electrical conductivity in the region $R_a < r < R$ will be zero. Electrical conductivity is proportional to temperature and modeled as follows [9]:

$$\sigma = \begin{cases} 0 & \text{se } T < T_e \\ \alpha (T - T_e) & \text{se } T > T_e \end{cases}$$

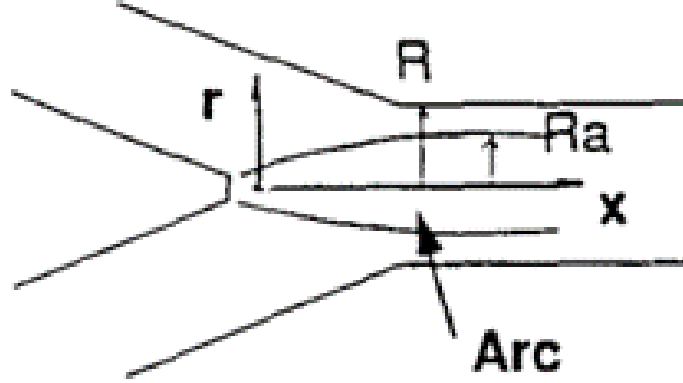


Figure 3.8: Representation of the dual channel model [9]

where T is the gas temperature, T_e is the average ionization temperature and α is the proportionality constant. The electrical conductivity value varies along the radial direction, in particular it is maximum at the center of the arc, for $r = 0$, and zero outside when $r = R_a$. By calculating an average value:

$$\bar{\sigma} = \frac{1}{2}\sigma_{MAX}$$

the current density in the central region will be:

$$j = \bar{\sigma}E$$

The electrical power deposited in the fluid is converted into thermal energy and conducted radially towards the edge of the arc. From the energy balance per unit of length it follows:

$$\frac{1}{2}\sigma_{MAX}E^2\pi R_a^2 = 2\pi R_a \left(k \frac{\partial T}{\partial r} \right)_{r=R_a}$$

The temperature gradient can be approximated as below:

$$-\frac{\partial T}{\partial r} \approx 2 \frac{T_c - T_e}{R_a}$$

where T_c indicates the temperature on the axis of the constrictor and T_e indicates the temperature on the edge of the arc; replacing the previous equation gives an expression for the electric field E as a function of the radius of the electric arc R_a :

$$E = 2\sqrt{2k \frac{(T_c - T_e)}{R_s^2 \sigma_{MAX}}}$$

or by substituting the expression of electrical conductivity in the form previously assumed:

$$E = \frac{2}{R_a} \sqrt{\frac{2k}{\alpha}}$$

Now, the total current inside the electric arc is defined by the current density which multiplies the area of the arc itself. Taking into account the variation of the arc radius along the axial direction of the thruster, we can express the electric current with the following integral:

$$I = \int_0^{R_a} 2\pi r \sigma E dr$$

Using once again the average value for the electrical conductivity and replacing the expression obtained for the electric field E the dependence on the radius R_a and the temperature T_c at the center of the electric arc is also obtained for the current I :

$$I = \frac{1}{2} \sigma_{MAX} \pi R_a^2 E$$

or

$$I = \pi R_a (T_c - T_e) \sqrt{2k\alpha}$$

The heat flow per unit area is transmitted from the arc column region to the surrounding flow. The balance of the energy exchanged at the edge of the electric arc is written below:

$$2k \frac{T_e - T_c}{R_a} = k_g \frac{T_e - T_w}{R - R_a}$$

where

T_w is the wall temperature and k_g is the thermal conductivity of the gas surrounding column arc. From the latter another form is obtained to express the difference between the temperatures at the center and at the edge of the arc. This form, substituted in the expression of the current, leads to:

$$I = \pi R_a \sqrt{2\alpha k} \frac{k_g}{2k} \frac{R_a}{R - R_a} (T_e - T_w)$$

It should be noted that the R_a that varies along the axial direction is not known a priori, while the value of the radius of the constrictor R will be assigned.

Multiplying the expressions obtained by the electric field and the current, a new form can be obtained to express the power per unit of length dissipated by the electric arc:

$$EI = 4\pi k (T_c - T_e)$$

This power is deposited in the propellant gas. Part of this gas reaches the temperature T_e and contributes to the growth of the electric arc. If we consider an infinitesimal length dx the power absorbed by the mass flow is:

$$4\pi k (T_c - T_e) = c_p (\rho u)_e 2\pi R_a \frac{dR_a}{dx} dx$$

where $(\rho u)_e$ indicates the mass flow at the edge of the arc and it must be estimated. So, under the assumption of 1D and non-viscous flow, the Bernoulli equation is valid and therefore in our case:

$$p + \rho u^2 = const$$

but if the pressure is independent of the radial direction at a given axial station then it is also legitimate to consider radius-independent ρu^2 . Furthermore, using the equation of state of ideal gases, the mass flow can be written as follows:

$$\rho u = \sqrt{\rho (\rho u^2)} = \sqrt{\frac{p (\rho u^2)}{\mathcal{R}T}}$$

Thus, we have:

$$\frac{(\rho u)_e}{(\rho u)_{out}} \simeq \sqrt{\frac{T_{out}}{T_e}}$$

where

$$(\rho u)_{out} = \frac{\dot{m}}{\pi (R^2 - R_a^2)}$$

and therefore

$$(\rho u)_e = \frac{\dot{m}}{\pi (R^2 - R_a^2)} \sqrt{\frac{T_{out}}{T_e}}$$

Now we can replace the latter in the power balance and we have:

$$\frac{\dot{m}}{\pi (R^2 - R_a^2)} \sqrt{\frac{T_{out}}{T_e}} R_a \frac{dR_a}{dx} c_p (T_e - T_{out}) \simeq 2k (T_c - T_e)$$

or by making the dependence on the current and on the arc radius appear in the second member and reworking the expression:

$$\frac{R_a^2}{R^2 - R_a^2} \frac{dR_a}{dx} \simeq \frac{I \sqrt{\frac{2k}{\alpha}} \sqrt{\frac{T_e}{T_{out}}}}{\dot{m} c_p (T_e - T_{out})}$$

To simplify calculations, we refer to non dimension quantities which we will indicate with an asterisk apex and which will be defined starting from the reference ones calculated from a priori known quantities.

For the reference current value we assume:

$$I_{ref} = \pi R \sqrt{2\alpha k} (T_e - T_w)$$

so

$$I^* = \frac{I}{I_{ref}}$$

Relating the radius of the electric arc to the radius of the constrictor taken as a reference dimension, the non dimension quantity is defined:

$$r_a = \frac{R_a}{R}$$

Furthermore, assuming that the thermal conductivity of the outer flow region is about half of the relative conductivity to the inner region, it is defined:

$$\lambda = \frac{k_g}{2k} \simeq \frac{1}{4}$$

Now, it is possible to find the link between the non dimension quantities I^* and r_a with fixed λ :

$$I^* = \lambda \frac{r_a^2}{1 - r_a}$$

The resolution of the second degree equation with respect to r_a leads to:

$$r_a^2 - \frac{I^*}{\lambda} r_a + \frac{I^*}{\lambda} = 0$$

$$r_a = \frac{2}{1 + \sqrt{1 + \frac{4\lambda}{I^*}}}$$

From the latter it can be seen that by increasing the current the value of R_a tends to one and this means that the electric arc occupies the entire passage section

of the constrictor.

With a similar reasoning, an expression for the electric field can be found. We define E_{ref} and therefore E^* is obtained:

$$E_{ref} = \frac{2}{R} \sqrt{\frac{2k}{\alpha}}$$

$$E^* = \frac{E}{E_{ref}}$$

or

$$E^* = \frac{1}{r_a} = \frac{1 + \sqrt{1 + \frac{4\lambda}{I^*}}}{2}$$

and from this you can see the typical behavior of the electric discharge or the negative voltage-current characteristic, in fact, as the current increases, the electric field and therefore the voltage decrease.

We also introduce:

$$x_{ref} = \frac{1}{2\pi} \frac{\dot{m}c_p}{k} \sqrt{\frac{T_{out}}{T_e}}$$

thus

$$x^* = \frac{x}{x_{ref}}$$

The power balance is written in non-dimension form:

$$\frac{r_a^2}{1 - r_a^2} \frac{dr_a}{dx^*} = \left(\frac{T_e - T_w}{T_e - T_{out}} \sqrt{\frac{T_w}{T_{out}}} \right) I^*$$

Since T_e is much larger than both T_w and T_{out} and the latter are of the same order of magnitude, the quantity in brackets to the second member can be approximated to one.

$$\frac{r_a^2}{1 - r_a^2} \frac{dr_a}{dx^*} \simeq I^*$$

Its integration allows to evaluate the R_a to R ratio as a function of x^* or in other words how the electric arc develops in the radial direction along the length of the constrictor. We denote the radius of the electric arc with $R_{a,L}$ in the exit section of the constrictor where the flow reaches the sonic condition. The mass flow rate will be:

$$\dot{m} = \Gamma \frac{p_{tot} \pi (R^2 - R_{a,L}^2)}{\sqrt{\mathcal{R} T_{tot}}}$$

Clearly \mathcal{R} is the universal gas constant while R is radius of constrictor, Γ is the function of Mach which for Mach equal to one is:

$$\Gamma = \sqrt{\gamma} \left(\frac{2}{\gamma + 1} \right)^{\frac{\gamma+1}{2(\gamma-1)}}$$

Also for the mass flow rate we introduce a reference value with respect to which we define the non dimension quantity:

$$\dot{m}_{ref} = \frac{p_{tot} \pi R^2}{\sqrt{\mathcal{R} T_{tot}}} \Gamma$$

and

$$\dot{m}^* = \frac{\dot{m}}{\dot{m}_{ref}}$$

carrying out the appropriate steps leads to:

$$\dot{m}^* = 1 - r_{a,L}^2$$

with

$$r_{a,L} = \frac{R_{a,L}}{R}$$

The voltage accumulated in the constrictor is:

$$V_{constr} = \int_0^L E dx = E_{ref} x_{ref} \int_0^{L^*} E^* dx^*$$

If we define:

$$V^*_{constr} = \frac{V_{constr}}{V_{ref}}$$

where we assume the denominator equal to the product $E_{ref} x_{ref}$. Remembering that:

$$E^* = 1/r_a$$

$$\frac{dr_a}{dx^*} = \frac{(1 - r_a^2)}{r_a^2} I^*$$

changing the integration variable we obtain:

$$V^*_{constr} = \int_0^{r_{a,L}} \frac{r_a}{(1 - r_a^2) I^*} dr_a$$

and solving:

$$V^*_{constr} = -\frac{1}{2I^*} \ln(1 - r_{a,L}^2)$$

It assumes that the arc growth is simply due to the flow expansion and, although attachment to the anode is a difficult problem to deal with, it is experimentally observed that the attachment point is downstream of the constrictor exit. On the basis of this we try to estimate the voltage drop in this region where the flow is supersonic. Looking at the Fig. 3.9 downstream of the constrictor, we see that:

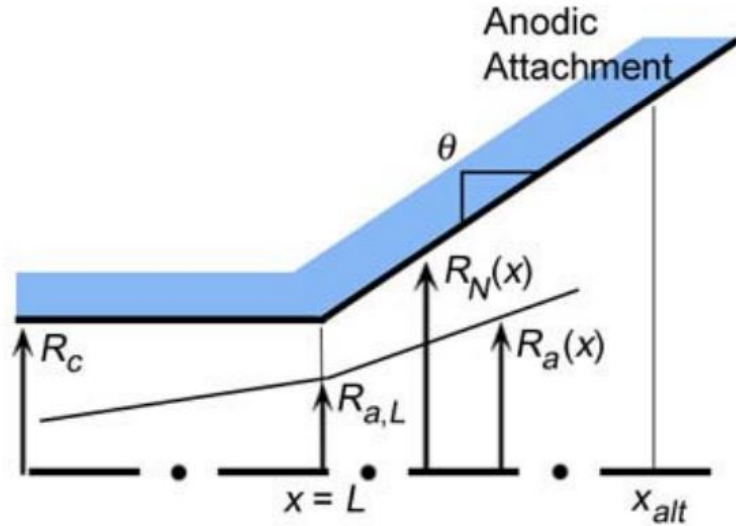


Figure 3.9: Representation of the electric arc growth [9]

$$R_a \simeq R_{a,L} \frac{R_N}{R_c}$$

$$dx = \frac{dR_N}{\tan \theta}$$

and remembering

$$E = \frac{2}{R_a} \sqrt{\frac{2k}{\alpha}}$$

we obtain:

$$\Delta V_{nozzle} \simeq 2\sqrt{\frac{2k}{\alpha}} \frac{1}{r_{a,L} \tan \theta} \ln \left(\frac{R_{N,att}}{R_c} \right)$$

It is also necessary to consider the voltage drop at the anode and cathode, the causes of which have already been discussed and empirical values will be assumed for these quantities.

3.4 Preliminary schematic design

The preliminary design of the arcjet provides for an electrical input power limited to a maximum of 1 kW. In paragraph 3.1 we discussed the analysis of different propellants and according to the first predictions it was mentioned that the choice of using water as a propellant is acceptable if the goal is set to reach a maximum of I_{sp} of 450 s. We now propose to conduct a nozzle geometry optimization process in order to meet the power requirement while achieving acceptable performance. The initial geometry was established on the basis of data from research on state-of-the-art arcjets. As already clarified, the I_{sp} is limited by the temperature that can be reached in the chamber due to the allowable heat flow near the walls of the nozzle and in particular in the constrictor. The throat diameter influences the pressure reached in the heating chamber and the minimum necessary mass flow for a stable operation of our electrothermal engine. Therefore, the throat diameter is the first of the parameters to vary in the optimization process. On the other hand, the variation in the length of the constrictor causes a variation in the length of the electric arc and therefore in the voltage-current characteristic of the arcjet. The erosion effects at the cathode tip have a greater magnitude with an increase in temperature and the latter increases with increasing current, so it would be good if the thermal arcjet thruster operated with high voltages and low currents. Then the dimension of the length of the constrictor constitutes another variable of this study. The third geometric design parameter was identified in the half cone angle of the divergent part of the nozzle. Its variation involves a variation in the pressure in the outlet section of the nozzle and in other words has an effect on the thrust. In this study, the geometric parameters identified are varied one at a time to grasp their influence on the performances and to find the optimum point for our engine.

The initial geometry is shown below:

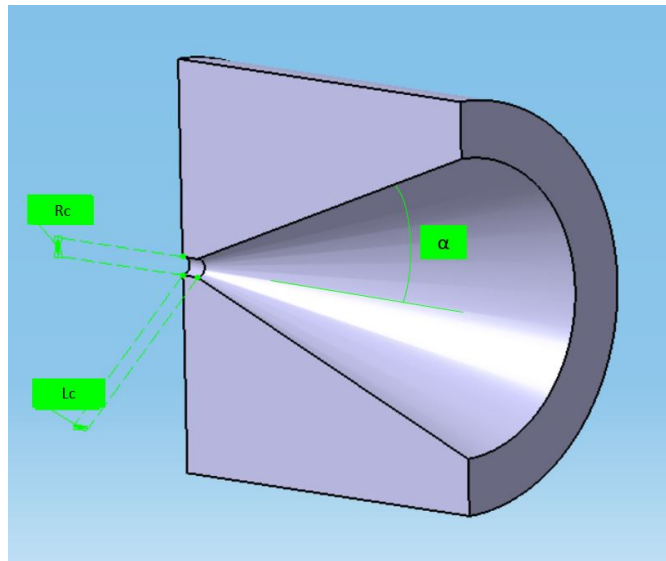


Figure 3.10: Geometry of nozzle

Table 3.2: Geometria

R_c [mm]	L_c [mm]	α [°]
0.6	0.7	20

Using the simplified analysis model introduced in the previous paragraph, the performance for different engine geometries can be evaluated. It is an iterative process whose starting point is given by the hypothesis of reaching a thrust of about 100 mN and a specific impulse of 450 s. On the basis of this and from the definitions of specific impulse and thrust, an initial propellant flow rate was estimated:

$$T = \dot{m}_p c$$

$$I_{sp} = \frac{c}{g_0}$$

where the effective discharge speed c is assumed to be approximately equal to the effective discharge speed u_e . With constant mass flow and thrust over time, it is obtained:

$$\dot{m}_p = \frac{T}{I_{sp} g_0} \approx 23 \text{ mg/s}$$

This initial estimate accompanied by fixed current values allow to evaluate the voltage and power operating of the engine. If geometry is given, the actual performance of the water-feed engine can be assessed.

Assuming an isentropic expansion of the flow starting from the throat section of the nozzle, it is possible to evaluate the Mach number in the outlet section for a fixed geometric expansion ratio:

$$\frac{A_e}{A_{ce}} = \frac{1}{M_e} \left(\frac{1 + \frac{\gamma-1}{2} M_e^2}{\frac{\gamma+1}{2}} \right)^{\frac{\gamma+1}{2(\gamma-1)}}$$

where A_e indicates the exit section of the divergent and A_{ce} indicates the exit section of the constrictor where the sonic condition is reached. Furthermore, the exit pressure is related to the stagnation pressure:

$$p_{tot} = p_e \left(1 + \frac{\gamma-1}{2} M_e^2 \right)$$

so, the thrust can be easily calculate by considering the exit plane as:

$$T = p_e A_e \left(1 + \gamma M_e^2 \right)$$

and the thrust efficiency will also be known from this. It is defined as the thrust power divided by the electrical input power as given in equation below:

$$\eta_T = \frac{T^2}{2\dot{m}_p P_{el}}$$

in this study, we try to optimize this parameter by changing the input variables and looking for a trade off between the electrical power required and the performance obtained to find the optimum point of the thruster.

3.5 Expected performance for the designed solution

To understand the influence of the nozzle geometry on the performance of the thruster, the throat diameter, the length of the constrictor and the half cone angle of the divergent part are varied with respect to the geometry taken as a reference[10]. The table lists the different cases that are analyzed:

Table 3.3: Geometry variation parameter

Nozzle	throat diameter [mm]	length [mm]	α [°]
1	0.6	0.7	20
2	0.6	0.7	19
3	0.5	0.7	20
4	0.5	0.4	20

The effect of the divergent angle can be understood from the comparison between nozzle 1 and 2. From the data shown in Tab. 3.4 it can be seen that to achieve the same specific impulse and thrust values, the thruster with a smaller cone angle would require more power. In other words, with the same power, the performance of the second engine and its efficiency are lower. This effect is explained by the fact that the pressure in the outlet plane is higher in the nozzle with a smaller divergent angle and the flow expands less causing a decrease in thrust.

Table 3.4: Performance data of nozzles 1 and 2

I [A]	V [V]	P [W]	η [%]
8	92.62	740.98	22.5
10	90.75	907.47	18.39
12	89.45	1073	15.55
8	93.16	745.28	22.39
10	91.27	912.71	18.28
12	89.96	1079.546	15.46

The nozzle 1 and the nozzle 3 have different constrictor diameter or cross section of the flow passage. With the same current, 10A, the voltage increases so that the

required power increases but in this case there is also an increase in specific impulse and thrust. This effect is caused by the fact that due to a smaller constrictor area, the pressure inside the combustion chamber increases and consequently the thrust is also greater. The table below lists the data obtained from nozzles 1 and 3 :

Table 3.5: Performance data of nozzles 1 and 3, $\dot{m} = 23mg/s$, $I = 10A$

I_{sp} [s]	T [mN]	P [W]	η [%]
407	91.9	881	21
409	92.34	1110.34	17

If the flow passage section is reduced, it is legitimate to think of a stable operation of the thruster with a lower mass flow rate. The reduction of the latter translates into a lower mass of propellant in favor of a greater mass of payload. Comparing the data for nozzle 3 and nozzle 4. in Tab. 3.6 you can see the effect of the length of the constrictor. At constant flow and current, the voltage of nozzle 3 increases, vice versa the latter for the same power level could operate at lower currents and higher voltages than nozzle 4 which has a shorter constrictor length.

Table 3.6: Performance data of nozzles 3 and 4, $\dot{m} = 18mg/s$, $I = 10A$

I_{sp} [s]	T [mN]	P [W]	η [%]
409.26	72.26	1014.4	14.3
407	71.9	791.23	18

In view of the above, the geometry of nozzle 3 appears to be the best compromise for final performance, therefore the defined parameters could be a good starting point for further analysis and future optimizations.

Finally, the geometry of the thruster was defined on the basis of statistical estimates on state-of-the-art arcjets and the sensitivity analysis of the geometric parameters of the nozzle. The data are summarized in the table below:

Table 3.7: Geometric arameters of the arcjet

Parameters	Value
Cathode diameter	3 mm
Constrictor length	0.7 mm
Constrictor diameter	0.5 mm
Divergent nozzle angle	20°
Convergent nozzle angle	80°
Electrode gap	0 mm

Chapter 4

Preliminary design

4.1 Preliminary design of a dedicated IOD satellite

The estimated performance for the arcjet is to be confirmed with numerical and experimental simulations, however in this section we want to define an In Orbit Demonstration IOD which aims to test the new propulsion system. The IOD / IOV , in orbit demonstration and validation, is a project that was created to overcome the so-called "Valley of Death", that is the gap between technological innovations and their commercial applications in the market.

- IOD refers to the space flight of a particular technology that would need further optimization to be adopted in space missions;
- IOV refers to the space flight of a particular technology for the purpose of its validation, so it can be understood as a step forward from the IOD.

To outline an IOD, it is necessary to describe the mission to be carried out, the platform to be used by considering the adaptation of existing ones such as dedicated spacecraft, autonomous systems for the distribution of multiple payloads, standardized platforms.

A new technology for space use is described by its maturity level as quantified by the Technical Readiness Level (TRL). The TRL is an integer on a scale from 1 to 9, originally defined by Nasa, and it is an index of the current state of the system as listed by the table:

Table 4.1: Definition of the Technical Readiness Level TRL [11]

TRL	Definition
TRL1	Basic principles observed.
TRL2	Technology concept formulated.
TRL3	Experimental proof of concept.
TRL4	Technology validated in lab.
TRL5	Technology validated in relevant environment (industrially relevant environment in the case of key enabling technologies).
TRL6	Technology demonstrated in relevant environment (industrially relevant environment in the case of key enabling technologies) .
TRL7	System prototype demonstration in operational environment
TRL8	System complete and qualified
TRL9	Actual system proven in operational environment (competitive manufacturing in the case of key enabling technologies; or in space)

The first step is to define the object of the mission which is clearly to test the functioning of the arcjet. The thruster must be capable of performing maneuvers such as station keeping, orbit and attitude control, deorbit maneuver, orbit raising. The performance of its functions is possible only thanks to other components that make up the propulsive subsystem of the space system. The arcjet must be supported by a power supply line, a propellant supply line and must be equipped with a thermal control system. The use of water as a propellant will also require the presence of a gas generator. The most critical components will be analyzed in the following paragraphs, while this section describes the platform identified as the most suitable for the in orbit demonstration.

The preliminary design of the arcjet began thanks to the data available on engines similar to the state of the art. The research has allowed us to estimate, in addition to the expected performance, also the dimensions and weight of the engine itself and this leads us to consider a CubeSat as the most suitable platform for IOD. CubeSats have become popular for various applications ranging from educational projects to scientific experiments or commercial applications, thanks to the relatively low cost of construction and launch. They are miniaturized cubic-shaped satellites with electronics made with Components Off The Shelf COTS, i.e., hardware and software components available on the market for acquisition by companies interested in using them in their projects. The initial standard of a CubeSats is a cube that is 10x10x10 cm in size and weighs of 1.33 kg. With the increase in demand, this platform has become 1 U, that is a unit, starting from which CubeSats up to 27 U

are made to have a greater availability of size and volume.

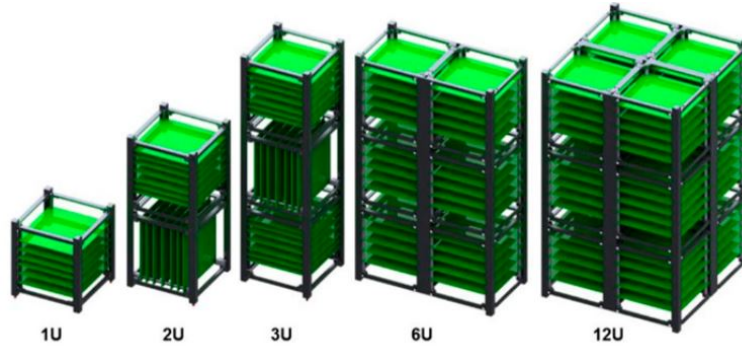


Figure 4.1: CubeSats size

The most suitable CubeSat for the IOD of the arcjet engine is 6U, the characteristics of which are shown in the table:

Table 4.2: Features of CubeSat platform with 6U

Size	6U
Dimensions	$20 \times 10 \times 34.5$ cm
Mass	$\sim 12kg$
Available Volume	up to 5U
Design Lifetime	5 years

Generally, a CubeSat has the same requirements and subsystems as any other satellite:

- Structure that must withstand loads, capable of resisting in the operating environment;
- Communication System (Comms) that helps in the tracking of the space segment by the ground segment, in providing and receiving telemetry and payload data. The payload is what interacts with the object of the mission, in our case the arcjet itself. The communication system consists of modem, transponder, filtering stage, diplexer, antennas and must receive / send data from the on-board computer in downlink / uplink communication. Typically

the frequency spectrum used in these applications is the UHF, VHF and S Band;

- Electrical Power System (EPS) which must generate electrical power, store it, distribute it, condition it and regulate it according to what is required by the other subsystems and by the various users on board. In the section 4.5 the power requirement imposed by the payload will be defined, which must be powered for a defined time for the completion of the maneuver in orbit;
- On Board Computer (OBC) that performs command and data handling and time keeping functions;
- Attitude Determination and Control System (ADCS) which allows you to maintain or change the orientation and therefore the angular velocity of the satellite so that it is stable during the implementation of the maneuver. In LEO orbits, the Earth's magnetic field can represent a source of disturbance for the attitude of the CubeSat which, subject to residual magnetization, will have its own magnetic dipole moment. The latter interacts with the Earth's magnetic field creating a disturb that must be compensated:

$$\mathbf{T}_m = \mathbf{M} \times \mathbf{B}$$

where \mathbf{T}_m is the magnetic torque, \mathbf{M} is the spacecraft magnetic dipole moment due to current loop residual magnetization in the spacecraft and \mathbf{B} is the Earth's magnetic field vector. The control is to be carried out with reaction wheels, flywheels set in rotation that exchange moment with the body of the satellite to counteract the disturbance. Mounted on the three axes, plus one in redundancy, they allow a high pointing but must be desaturated and then coupled to magnetorquer. For the determination of the attitude or measurement of the angular velocity, the use of sun sensors coupled to gyroscopes is essential for the satellite detumbling phase, an adjustment maneuver immediately after the satellite is released, in which the sun sensors are not effective.

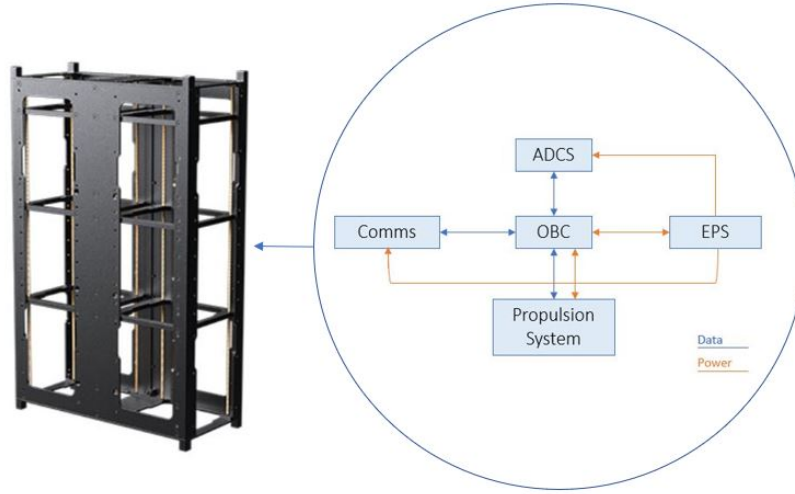


Figure 4.2: Satellite subsystems assembly

Once the platform, including its subsystems, which can be equipped by the arcjet has been identified, it is decided to evaluate the performance of the engine in an orbital raising maneuver. The choice of orbit affects the mission in several ways. A satellite in eclipse must be powered based on the amount of energy stored in the batteries, in the phases of daylight it is subject to greater thermal loads and all components must be kept within the allowable temperature ranges, the altitude of the orbit determines the environment in which the segment operates and the disturbances it will address. In LEO the atmospheric resistance of the Earth causes a greater decay of the orbit. Orbit decay has become an important factor in the space environment. The European Code of Conduct for Space Debris Mitigation requires the satellite to be deorbited within 25 years, this could help avoid unwanted collisions in space. When the spacecraft travels in the sphere of influence of the Earth it suffers the force due to the drag that opposes its motion [12]:

$$D = \frac{1}{2} \rho v^2 A_S C_D$$

where A_S is the cross-section area of the CubeSat, C_D is the ballistic coefficient that we can assume equal to 2.2. From Kepler's third law we can evaluate the orbital period P :

$$P^2 GM_E = 4\pi^2 a^3$$

where G is the Universal Gravitational Constant, M_E is the mass of the Earth and

a is the semimajor axis which in the case of circular orbits is simply the radius of the orbit. The variation of the orbital period due to atmospheric resistance will be:

$$\frac{dP}{dt} = -3\pi a \rho A_s C_D / m_s$$

with m_s is the satellite mass.

For the calculation of the atmospheric density the NASA atmospheric density model was considered [13]:

$$\rho = \frac{p}{(0.2869(T + 27301))}$$

where the temperature and pressure are:

$$T = -131.21 + 0.00299h$$

$$p = 2.488 \left(\frac{T + 273.1}{216.6} \right)^{-11.388}$$

By coupling and implementing the equations in a Matlab code, it has been seen that the cubesat chosen for the IOD complies with the requirement of the ESA code if it orbits in LEO at a height of about 450 km from the Earth. If the maneuver is opposite or rather than deorbiting the satellite you want to do an orbit raising from 450 km to 550 km considering circular orbits, the initial and final speeds can be calculated:

$$v_i = \sqrt{\frac{\mu}{r_i}} = 7.64 \text{ km/s}$$

$$v_f = \sqrt{\frac{\mu}{r_f}} = 7.585 \text{ km/s}$$

where r_i and r_f are the initial radius and the final radius of the orbit, i.e. the sum of the radius of the Earth and the height h . Therefore

$$\Delta v = v_f - v_i = 55.343 \text{ m/s}$$

From the Tsiolkosky equation it is possible to calculate the mass of propellant necessary to carry out this maneuver:

$$m_p = m_0 \left(1 - e^{-\frac{\Delta v}{c}} \right)$$

where the initial mass m_0 is the mass of the satellite at the start of the mission. Thus

$$m_p = 168.11g$$

this value will allow us to size the tank and will be discussed below. We can understand the time required for the maneuver from the estimated flow rate in the analysis of the arcjet performance and from the propellant mass just calculated:

$$\Delta t = \frac{m_p}{\dot{m}_p} \approx 2.5h$$

4.2 Evaporator

The use of a conventional propellant feed system for a high-power arcjet in which the gas generator is directly coupled to the engine could cause various problems. A typical vaporizer adopted in the propellant feed system of the high-power arcjet is larger and heavier than that required by the low-power arcjet since the flow rates involved are lower. A downsizing of this component is not enough to solve the problems since by directly coupling the vaporizer to the thruster you can see an instability in the flow of gas supplied to the engine with a consequent reduction in performance.

A liquid flowing in a channel and needs to be vaporized is heated in its liquid phase to the point where the nucleation of the bubbles first occurs [14]. The boiling of the nucleated continues until enough steam is generated that the resulting increase in velocity is sufficient to suppress nucleation. Beyond this point, heat is added to a thin liquid film and vaporization occurs at the liquid-vapor interface. During these boiling regimes, the liquid is drawn into the vapor core. Despite the eventual redeposition of liquid from the core to the film, at a certain point there is no longer enough liquid to wet the wall. The liquid film breaks with a large reduction in the heat transfer coefficient. The phenomenon described is represented in Fig. 4.3.

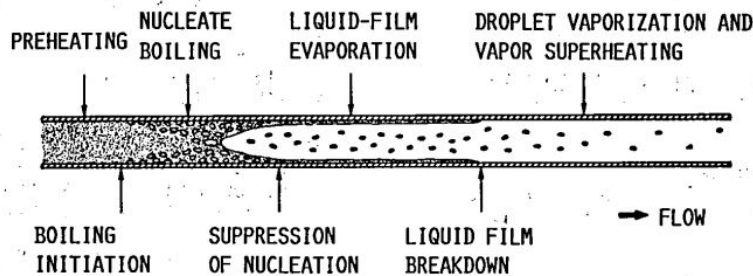


Figure 4.3: Typical heat-transfer regimes for boiling in flow channel [14]

To solve the fluctuations of flow rate to which the arcjet is very sensitive, a gas plenum in communication with the gas generator accumulates the gas propellant from the gas generator at the desired pressure. A check valve actively controls propellant to the gas generator and the control valves upstream and downstream of the gas plenum control the flow of gas from the vaporizer and to the thruster. In this way it is possible to ensure a substantially continuous flow rate of gas propellant which feeds the arcjet.

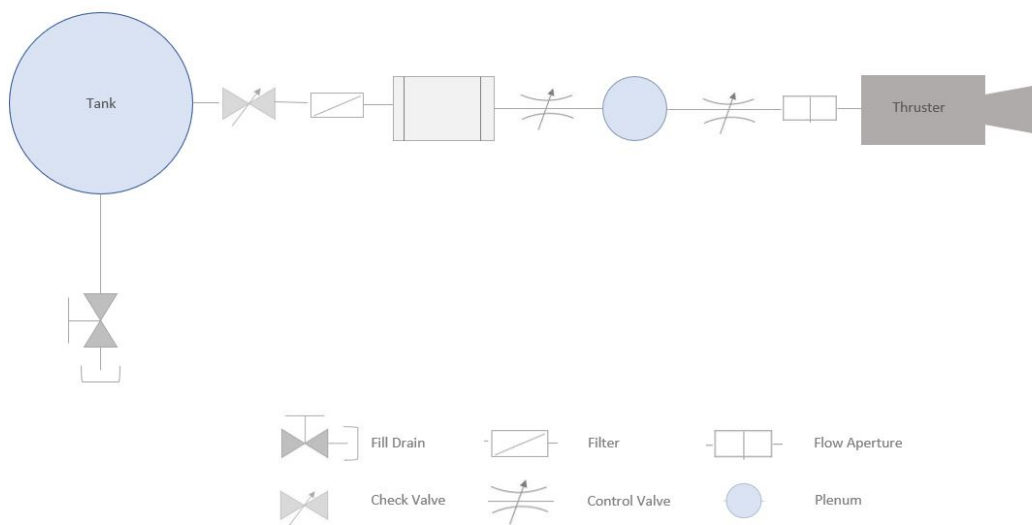


Figure 4.4: Sketch of propellant feed system

The vaporization mechanism used consists in heating a component that makes up the core of the vaporizer, this central unit heats the entire component so that the heat is then transferred to the propellant liquid. This concept has so far been implemented in several ways. In Fig.4.5 you see a gas generator in which there is a heating unit that heats the entire stainless steel component. The heat is conducted from the inner core to the liquid propellant coming from the tank and flowing through helical channels. This component was tested for the vaporization of liquid ammonia that was to feed the thermal arcjet Talos.

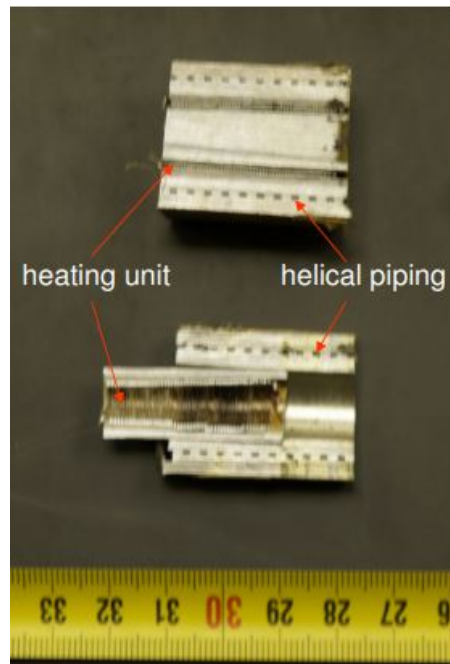


Figure 4.5: Vaporizer Concept for Ammonia [15]

[15] Under zero gravity conditions, the propellant drops may not be in direct contact with the hot walls of the channels with very poor vaporization efficiency. This has led to a search for more efficient heat exchange. A first example is shown in Fig. 4.6. The difference lies in the heating unit which is integrated into the passage channel and a stainless steel scrub coiled around it. In the research conducted for

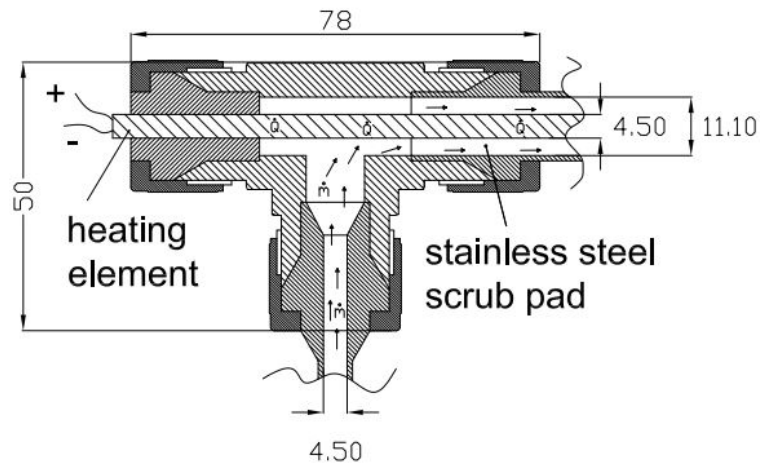


Figure 4.6: Gas generator adopted by Talos arcjet [15]

this study, another prototype of gas generator developed specifically to vaporize water appeared. This concept is shown in Fig.4.7 As you can see it uses a heat glow plug, latter is used for car diesel engines as a heater, reached 1100 degrees Celsius in about two seconds, and the tip becomes red-hot.

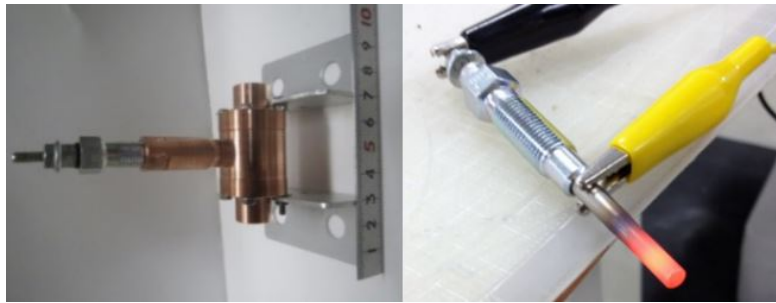


Figure 4.7: Prototype of gas generator for water [16]

For an estimate of the desired heating power for a complete vaporization of the propellant liquid, it is possible to refer to the following equation:

$$\dot{Q} = -\dot{m}_p c_p (T_{in} - T_{out})$$

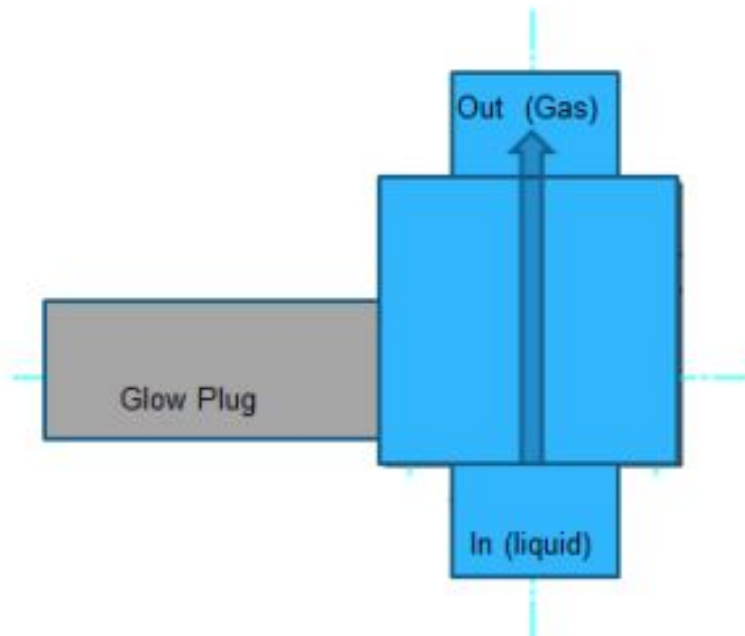


Figure 4.8: Skech of gas generator concept [16]

where \dot{Q} is the heating power, \dot{m}_p is the propellant mass flow, c_p is the specific heat and $(T_{in} - T_{out})$ is the temperature difference between the inlet and outlet. Assuming a mass flow of 18mg/s , a temperature difference of 800K and a specific heat of 4615J/(kgK) , the necessary power results of 66.5W and with a margin of 10% the requirement for the heating power of the vaporizer is set to 73W .

4.3 Tank

The simplest way to feed the thruster is to move the propellant from its storage tank using a pressurant gas. An alternative way is the use of a pump driven by turbines or electric motors. Generally, systems with pressurant gas are used when the thrust and total impulse levels are low because, having the tank withstand a pressure higher than the pressure in the engine chamber, they tend to be heavier than pump-fed systems. If the thrust request increases and consequently also the necessary propellant mass increases, the tank pressure linked in turn to the pressure in the chamber increases to the point of making the weight of the tanks prohibitive. The management of a liquid propellant in space is complicated by the absence of gravity. Several technological concepts of tanks are employed on satellites today and can be divided into two groups:

- Propellant Management Devices PMDs: the surface tension is exploited to separate the liquid propellant from the gas;
- Positive Expulsion Devices PEDs: they use an active element to separate the pressurant gas from the propellant liquid.

In PMDs tanks the main parameter is the behaviour of the liquid on the surface of the component. This parameter depends on the contact angle which below 90° defines a wetting behaviour and liquid will flow along corners, an effect that can be achieved with various types of PDMs such as vanes, screens and sponges. To function efficiently enough, the contact angle must be less than 30° , but it is known that this condition does not occur for water that has a high surface tension.

In PEDs, liquid and gas are generally separated by a diaphragm, piston or bellows. The operation is based on the expansion of the pressurant gas that pushes the liquid propellant towards the supply line. By adopting a blowdown configuration, shown in Fig.4.9 the liquid propellant and the pressurant gas are in the same tank. When the valve is opened, the liquid propellant is pushed towards the outlet of the tank by the expansion of the pressurized gas.

For the sizing of the tank we assume that it is spherical shape. The total tank volume is the sum of the total volume of the propellant and the volume of the initial pressurant gas which are linked by a so-called blowdown ratio:

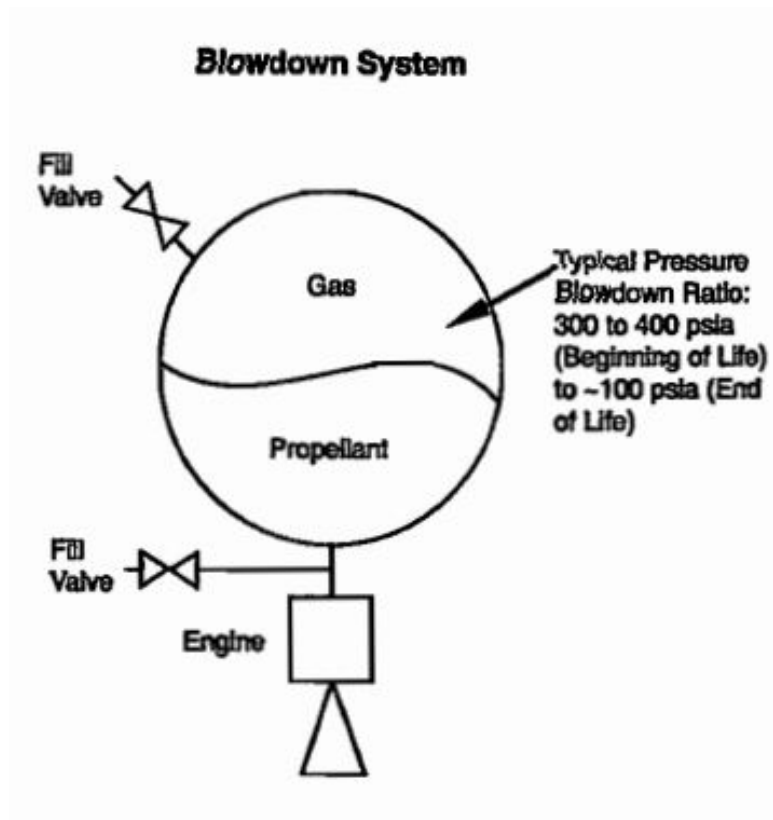


Figure 4.9: Blowdown system [17]

$$B = \frac{V_{gf}}{V_{gi}} \approx \frac{V_{gi} + V_p}{V_{gi}}$$

where V_p is the total of the propellant volume, V_{gi} is the initial gas volume in the tank and V_{gf} is the final gas volume, neglecting the propellant volume remaining at end-of-life. It is necessary to consider a design margin for the propellant load which has been statistically estimated to be around 25% plus 5% due to the residual propellant. Note the mass of water propellant necessary for the raising maneuver, the volume of water is evaluated in the initial conditions with the ideal gas law.

Table 4.3: Characteristics of the water propellant

T_0	298	K
ρ	997	Kg/m ³
V_{usable}	0.17	1

where V_{usable} is the volume of water that is actually needed. Adding the design margin to the volume of water:

$$V_p = V_{usable} + 30\%V_{usable} = 0.22l$$

The radius of the tank is calculated by imposing a spherical volume, then it is obtained:

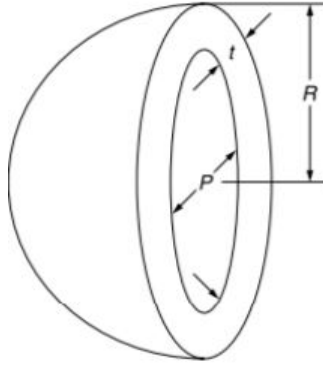


Figure 4.10: Section of spherical tank

$$V_p = \frac{4}{3}\pi R^3$$

$$R = \sqrt[3]{\frac{V_p}{\frac{4}{3}\pi}} = 3.43cm$$

To calculate the mass of pressurant gas, reference is made to the blow-down ratio generally variable between 3 and 6. We assume an average value of 4.5 and we evaluate the volume occupied by the gas at the beginning of the expansion or before carrying out the maneuver.

$$V_{gi} = \frac{V_p}{B - 1} = 0.06l$$

Helium is generally used as a pressurizing gas because it is the second lightest element after hydrogen with respect to which it also has the advantage of being inert. The pressure to which the gas is subjected is the maximum expected operating pressure, p_{MEOP} , in the tank. This pressure value was set at 1.2 MPa consistently with the data found in the literature. Therefore the gas mass in the tank is simply

calculable:

$$m_{He} = \frac{p_{MEOP} V_{gi}}{\mathcal{R}T_0} = 0.12g$$

Usually, we select the material, estimate the tank size, determine the thickness from the equation:

$$\sigma = \frac{p_{MEOP} R}{2t}$$

where σ is the allowable stress and t is the thickness. Generally, the constituent material of the tank walls is titanium alloy Ti-6Al-4V whose characteristics are shown below:

Table 4.4: Density and tensile strength of tank material

Parameter	Value	Unit
σ	833	MPa
ρ	4430	Kg/m ³

Having estimated the radius of the tank and introducing the safety factor, the thickness of the tank is evaluated:

$$t = \frac{C_S R p}{2\sigma} = 0.03mm$$

At this point it is easy to estimate the weight of the tank alone:

$$m_t = \rho V_t = 2.02g$$

the total weight of the tank necessary for the mission will be the sum of the weight of the propellant, the weight of the pressurant gas and that of the tank in which they are contained:

$$m_{TOT,tank} = m_p + m_t + m_{gi} = 170.25g$$

A spherical tank can withstand pressure loads better than any other shape, allowing thin tank walls and a light design. On the contrary, however, this design provides a very inefficient shape for the use in the rectangular area within the CubeSat. However, the general sizing reported here has the purpose of providing the order of size of the size and weight of the tank, but it is always possible to optimize the project in a more advanced phase of its definition.

4.4 Thermal control

The role of the thermal control subsystem is to keep the S / C, its subsystems and its components within the limit temperatures for each phase of a space mission. The limit temperatures that must be considered define two different ranges:

- Operational limits, temperature range in which the component must remain for its entire operational life;
- Survival limits, temperature range in which the component must remain all the time, even when it is not powered.

It is intuitive to understand that the survival temperature range is of fundamental importance since if these limits are not respected, permanent damage to the component can occur which can also compromise the general functioning of the system. The limit temperatures are a cold temperature which must not be lowered and a hot temperature which must not be exceeded. Typical examples of the thermal requirements to be met for the different components of an S / C are listed in Tab.4.5

Component	Typical Temperature Ranges (°C)	
	Operational	Survival
Batteries	0 to 15	-10 to 25
Power Box Baseplates	-10 to 50	-20 to 60
Reaction Wheels	-10 to 40	-20 to 50
Gyros/IMUs	0 to 40	-10 to 50
Star Trackers	0 to 30	-10 to 40
C&DH Box Baseplates	-20 to 60	-40 to 75
Hydrazine Tanks and Lines	15 to 40	5 to 50
Antenna Gimbals	-40 to 80	-50 to 90
Antennas	-100 to 100	-120 to 120
Solar Panels	-150 to 110	-200 to 130

Table 4.5: Typical thermal requirements for spacecraft components. [17]

Thermal control is applicable in different ways grouped into two categories:

- Passive thermal control, based on the use of specific materials, coatings or surface finishes;
- Active thermal control, based on the use of components that require a power supply.

For the design of the thermal control system it is first of all necessary to identify the constraints and requirements of the component with particular attention to its

specifications and any problems that may arise from it such as prolonged ignition of the engine which can cause significant heating by radiation of the neighboring surfaces. It is also necessary to know the global thermal environment in which the S / C operates and identify the sources of heat external to it. The major source is always direct solar radiation, the solar constant is $1367W/m^2$ which has been evaluated as an average over the solar year. The flow of heat due to the activity of the Sun depends on the absorptivity of the surfaces, the frontal area, the time of view and thus the orbit. In addition to solar radiation, the Earth itself or other celestial bodies affect the thermal load that impacts the system. Once the external heat sources have been identified, it is necessary to compare them with the requirements and constraints and identify the critical situations in which to design the thermal control system. The critical situations are the two worst cases: the hot case, where the S / C is directly exposed to the activity of the Sun and there is the maximum dissipated power; the cold case, when the S / C is in eclipse and there is the minimum dissipated power. In the case of our propulsion system, the temperature ranges that must not be exceeded will be different for the liquid and gaseous phase in which the water is in the components that make up the propulsion system such as the tank and the evaporator. The water tank must be kept at a nominal operating temperature equal to the ambient one, i.e. the temperature limits must be the freezing point, below which it must not fall, and the boiling temperature, which must not be exceeded. Therefore the tank will be coupled to heaters and temperature sensors. Heaters are used in thermal control design to protect the tank component under cold-case environmental conditions or to make up for heat that is not dissipated. On the other hand, for the arcjet thruster, the use of active thermal control hardware such as colplates is expected. A cold plate is a fluid flow space that is contained within bounding metallic walls. The key task is to design fluid flow passages within the space such that the heat dissipated by the thruster is extracted while maintaining temperatures at a level compatible with high performance. This thermal control system extracts heat from the component, leading it to the external circuit of the thermal control system in charge of rejecting the heat towards deep space.

4.5 Power supply subsystem

To operate the arcjet thruster properly, the power processing unit, PPU, must supply conditioned voltage and current at a constant average power level. To maintain the required average power level, the PPU must monitor the arc voltage and adjust the output current accordingly. For a low power arcjet the PPU is similar to that used on any other satellite equipped with an high or medium power arcjet. The general requirements of the PPU are the same:

- High efficiency
- Low Mass and Volume
- Radiation Hardness
- High reliability

During the operation of the propulsion system, the PPU receives electrical power and commands from the on-board satellite system. In turn, it supplies conditioned power to the thruster and thruster status and telemetry data to the on-board computer. The PPU also provides real-time control of the arcjet based on external commands from the ground based satellite controller. A DC to DC converter inside the PPU must manage the voltage level required by the engine with respect to the internal voltage of the satellite of about 28 Volts. The voltage-current characteristic of the PPU must have a greater slope than the arc characteristic to ensure its stability for any propellant flow rate value, as shown in Fig. 4.11

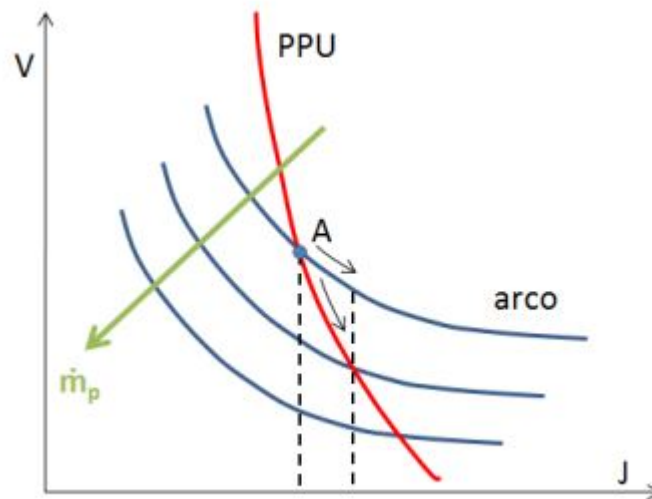


Figure 4.11: Voltage-current characteristics of arc and PPU. [1]

Suppose that point A is the operating point of the arc-PPU system. With any disturbance that causes an increase in the current, the PPU acts to decrease the voltage and the current of the electric arc returns to its initial operating point. Finally, it will have to tolerate current fluctuations, the so-called ripples. Time-varying currents generate electromagnetic waves that can interfere with telecommunication systems or other systems of S / C. The PPU represents the

most expensive and heaviest element of the entire propulsion system, a typical characteristic value for a PPU of an arcjet is 2.5 kg / kW, unfortunately the it is larger and heavier than the electrothermal arcjet itself.

A S / C orbiting the Earth, from LEO to GEO orbits, uses photovoltaic cells as energy sources by exploiting the greater solar radiation in these space environments compared to satellites operating in interplanetary missions. To size and define the arrangement of the solar panels, it is necessary to know the configuration of the S / C as well as the required power level and the orbit, including daylight and eclipse time. Once the amount of power to be produced has been calculated and the type of solar cell selected, the power output from the cell is estimated as a function of the incident radiation and the efficiency of the cell itself. Finally, taking into account the degradation factor of the cell, the area of the solar array necessary to produce the required power is calculated based on the power at the end of life P_{EOL} . Energy is stored through batteries which are defined as "primary", non-rechargeable, and "secondary", rechargeable. The battery voltage depends on the amount of cells in series, while the current increases with more cells in parallel, the net result is the battery capacity level. The dimensioning of the EPS goes beyond the definition of the IOD for our engine, in other words the energy required for the demonstration of this new technology is within the requirements. The estimated maneuver time Δt multiplied by the 1 kW power required for operation of the arcjet provides the value of the energy required:

$$E = P\Delta t = 2544Wh$$

Chapter 5

Conclusions

This thesis was aimed at defining the preliminary design of an innovative arcjet project that could be a competitive product in the space market.

The choice of the propellant was based on the estimate of the ideal performances and the advantages brought not only to the entire mission but also on the operating environments. The use of an inexpensive and green propellant such as water ensures the space safety and cost savings.

The theoretical model applied made it possible to identify the geometric parameters of the nozzle that play a key role in the performance that can be achieved. The result of this analysis was the design of a nozzle that optimizes arcjet operation. Despite the requirement to be imposed on the gas generator which shall provide a constant flow rate to the engine, sensitive to fluctuations, the arcjet can provide a specific impulse of the order of 400 s. The computational model applied led to real performance estimates that are expected to be tested in orbit. For this purpose, a preliminary dimensioning of the components of the propulsion subsystem was carried out.

Finally, the further objective achieved in this work was the identification of the CubeSat 6U platform and of the other subsystems necessary for the in-orbit demonstration of the arcjet.

Bibliography

- [1] Cristiano Pizzamiglio Prof. Lorenzo Casalino. «Propulsione Spaziale». In: A.A. 2013-14 (cit. on pp. 6, 8–11, 61).
- [2] Lingyun Hou, Yan Shen, Huangzai Tang, and Wenhua Zhao. «Improvement on stability of water arcjet». In: *IEEE Transactions on Plasma Science* 39.1 (2010), pp. 608–614 (cit. on p. 7).
- [3] Casalino L. *Space Propulsion*. 2020 (cit. on pp. 14, 18, 19).
- [4] Kristof Holste et al. «Ion thrusters for electric propulsion: Scientific issues developing a niche technology into a game changer». In: *Review of Scientific Instruments* 91.6 (2020), p. 061101 (cit. on p. 16).
- [5] Robert G Jahn. *Physics of electric propulsion*. Courier Corporation, 2006 (cit. on p. 22).
- [6] Hai-Xing Wang, Jin-Yue Geng, Xi Chen, and Wenxia Pan. «Numerical simulation of a low-power hydrazine arcjet thruster». In: *Physics procedia* 32 (2012), pp. 732–742 (cit. on p. 27).
- [7] Darrel Kim Robertson. «Simulation and design of a hydrogen arcjet thruster seeded with cesium». PhD thesis. Massachusetts Institute of Technology, 2001 (cit. on pp. 28, 30).
- [8] Manfred Ehresmann, Jonathan Skalden, Martin Fugmann, Stefanos Fasoulas, Sabine Klinkner, Isil Sakraker, Tina Stähler, and Oliver Refle. «Iras: low-cost constellation satellite design, electric propulsion and concurrent engineering». In: (2018) (cit. on p. 29).
- [9] M MARTINEZ-SANCHEZ. «Simplified Analysis of Arcjet Operation, Lecture 11-12, 16.522 Space Propulsion». In: *Aeronautics and Astronautics* (2004) (cit. on pp. 31, 32, 38).
- [10] Dagmar Bock, Monika Auweter-Kurtz, Helmut L Kurtz, and Hans-Peter Röser. «Experimental Investigations on Thermal Arcjet Thruster Development for a Science Mission to the Moon». In: *57th International Astronautical Congress*. 2006, pp. C4-4 (cit. on p. 42).

- [11] EU (European Union) and G. Technology Readiness Levels (TRL). *Horizon 2020—Work Programme 2014–2015: General Annexes*. 2014 (cit. on p. 46).
- [12] Colum Walter. «Development and Definition of a CubeSat Demonstrator for a Water Propulsion System». PhD thesis. Universität Stuttgart, 2021 (cit. on p. 49).
- [13] TP Brito, CC Celestino, and RV Moraes. «Study of the decay time of a CubeSat type satellite considering perturbations due to the Earth’s oblateness and atmospheric drag». In: *Journal of Physics: Conference Series*. Vol. 641. 1. IOP Publishing. 2015, p. 012026 (cit. on p. 50).
- [14] WEARL MORREN and JAMES STONE. «Development of a liquid-fed water resistojet». In: *24th Joint Propulsion Conference*. 1987, p. 3288 (cit. on p. 51).
- [15] Dagmar Bock, Monika Auweter-Kurtz, Georg Herdrich, Helmut Kurtz, and Hans-Peter Röser. «An advanced ammonia propellant feed system for the thermal arcjet TALOS». In: *43rd AIAA/ASME/SAE/ASEE Joint Propulsion Conference & Exhibit*. 2007, p. 5186 (cit. on p. 53).
- [16] Y Nogawa and H Tahara. «Evolutional Electrical Propulsion with Water Propellant DC Arcjet». In: *35th International Electric Propulsion Conference*. 2017, pp. 2017–413 (cit. on p. 54).
- [17] Jason R. Wertz Wiley J. Larson. *Space Mission And Design*. Space Technology Library, 1992 (cit. on pp. 56, 59).